
Dear editors,

There is a response to reviews of our manuscript “Insights into a historic severe haze weather in Shanghai: synoptic situation, boundary layer and pollutants” (acp-2015-665). We thank very much for anonymous reviewers, and their suggestions are helpful for improving our manuscript. According to reviewer’s suggestions, we make revision to the manuscript in detail, all of revision have been marked in red in the new manuscript. The following is a point-to-point answer to comments.

For Referee 1

Question 1: The paper compared several controlling factors for their correlations with visibility.

These factors include RH, PM, and particle number concentration at different sizes. However, these correlations were not based on the physical relationships. Directly computing the correlation coefficients for visibility (km) may not be appropriate, because the visibility values are generally low during hazy days and the correlation coefficient would be largely determined by the high visibility data. The authors could consider using the inverse of visibility as a proxy of extinction coefficient (at ambient RH) to do such analysis.

Answer: The extinction parameter can be converted to Vis using an equation such as from Stoelinga and Warner (1999) as $Vis. = -\ln(0.02)/Ext.$ (Stoelinga M.T. and Warner T.T. Nonhydrostatic, mesobeta-scale model simulations of cloud ceiling and visibility for an East Coast winter precipitation even, *Journal of Applied Meteorology*, 1999, 38: 385-404). However, in this paper, Vis. is used for a direct proxy of haze identification, influenced by various factors of particle mass (PM_{2.5}), RH, particle number and sizes, particle chemistry, etc. We have analyzed the correlations between Vis. and these factors to only understand their possible linking or contributions to haze formation. In the next paper, we will make a deeper analysis of their relationships using data of Sca and Abs parameters measured by nephelometer, cavity ring-down spectroscopic instrument and aethalometer.

Question 2: The authors used the measured inorganic ions to calculate the hygroscopicity. The contribution of water-soluble organic carbon (WSOC) was entirely omitted in this analysis. WSOC can contribute 5%-40% percent of the water content for urban aerosols, depending on the particle size and composition. The value of kappa was therefore underestimated. In addition, the authors simply added sulfate, nitrate, and ammonium ions and assigned a kappa value of 0.6 (ammonium sulfate) to this group. This treatment was somewhat oversimplified. In some conditions, the bisulfate or sulfuric acid can present when the particles are acidic. The contribution of H⁺ to hygroscopicity would be omitted in this simplified treatment. Although this may not be the case for current study (because the concentration of nitrate is high, as an indication of excess ammonium), the method used in current manuscript can be very misleading for readers. The data should be analyzed in a more rigorous way, e.g., by considering ion balances or using a thermodynamic model.

Answer: It is notable that the contribution of water-soluble organic carbon (WSOC) shouldn't be ignored in estimating values of hygroscopicity. In fact, the contribution (percent) of WSOC to hygroscopicity varies highly with time and region. In this paper, we simply considered sulfate, nitrate, and ammonium ions and assigned a kappa value of 0.6 (ammonium sulfate) to this group because of a lack of the available data of organic carbon during this period. The value of kappa

maybe somewhat underestimated. On the other hand, we mainly aimed to estimate the potential influence of RH to atmospheric visibility impairment by evaluating the contribution of inorganic ions to hygroscopicity. In the following paper, we will take more focuses on the impacts of particle chemistry and mixing or aging to hygroscopicity including a thermodynamic model. We have added some description about it in the revised manuscript.

Question 3: CCN data. For about half of the CCN data shown in Fig. 6, the CCN number concentration for 0.2% SS is higher than that for 0.4% SS.

Answer: It's really a fatal mistake that we neglected to select the valid CCN data of each supersaturation. The continuous-flow CCN counter (CCN-100) manufactured by Droplet Measurement Technologies (DMT, USA) was utilized to measure the CCN activation concentrations. Five supersaturations (e.g. 0.2, 0.4, 0.6, 0.8, and 1.0%) made up a cycle of half an hour, taking 10 min for 0.07% and 5 min for other supersaturations. Between the switch of different two supersaturations, it need a short period time to change into stable situation and the data should be abandoned. Therefore, that is we ignored before which is fatal to the result. We have corrected this mistake in the new figure 6. The figure shows as below.

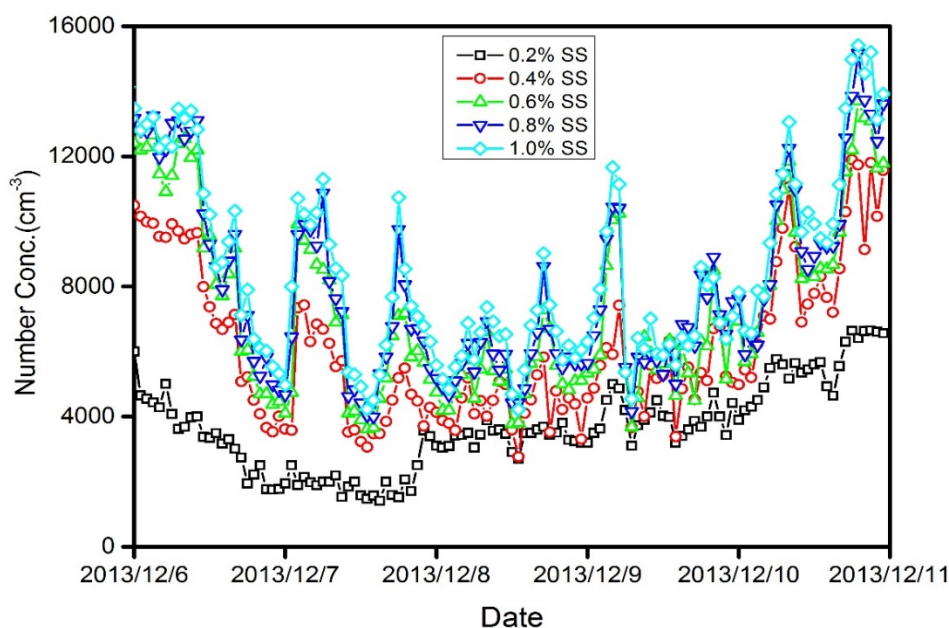


(Figure 6: Time series of 1-h mean CCN concentration (N_{CCN}) at supersaturations (SS) of 0.2-1.0% from 6 to 10 December.)

Question 4: Criteria of haze. In section 3.1.1, the authors state that " It has been widely accepted that the key criterion for discerning a haze event is to identify an apparent decrease of atmospheric visibility less than 10 km, and ambient relative humidity (RH) below 80% lasting for several hours (Fu et al., 2008; Du et al.,2011). When $80\% < RH < 90\%$, the event is referred to as a complex of haze-fog co-occurring or transition, and it is also classified into hazy episode in the present study (Leng et al., 2014a)."These definitions are vague and not widely accepted. A classification guideline for fog and haze using RH and visibility might be acceptable as an operational definition.

Answer: We agree with you that the definitions of criterions for discerning a haze event are vague

and not widely accepted. We just use these criteria to classify fog and haze events. In recent years in China, our government pays great attention to the environmental issues which are really thorny problems, and the document of haze pollution discriminant standard (trial) has been compiled by many researchers in China. Therefore, we use RH and visibility as an operational definition to discern haze events. Furthermore, we are inclined to consider other additional data (like PM_{2.5}) to discern. We have added more description in the new manuscript about it.

Minor comments:

Question 5: Abstract: the abstract should be revised. Please use short and clear sentences to improve the readability.

Answer: We have revised the abstract in the new manuscript.

Question 6: The language, in particular terminology, should be carefully checked throughout the whole manuscript to ensure that it is precise. Here are a few examples: ...

Answer: We thank you for your good comments and suggestions, and have specified them in our revised manuscript.

Question 7: **Section 2.2.** Specify the principle of MAGRA. Are the gases measured by MAGRA also analyzed? Was the size distribution measured at dry condition? "LPS was calculated ..." How LPS was calculated? By Mie model? Or it is just a calibration using the PSL particles? "Without obscuration due to relatively lower aerosol loading and well mixed atmosphere". What does this sentence mean? Why lower aerosol loading can obscure the atmosphere? Specify the operation principle of PM monitors. Does the RH affect the measurements?

Answer: The principle of MARGA has been added in the paper using red highlight. The data has been compared with other teams in our department before used, revealing the relative error was within 10% for SO₄²⁻ and NH₄⁺. The hourly-averaged conc. of gases was from the Shanghai Environmental Monitoring Center (SEMC), which was measured by the precision instruments. For the WPS, of course, aerosol flow passes through a silica-gel Diffusion Drier before getting into the WPS. In that case, the relative humidity can be controlled. According to the user manual, we learn the theory of WPS and the description of LPS theoretical response calculation is described as follows. "The LPS infers the particle size distribution from measurements of light scattering. It draws an aerosol into a sensing chamber, where the aerosol is illuminated with a beam of laser light. The light scattered by the aerosol is then collected by a photomultiplier tube. The amount of scattered light is then proportionally converted into a voltage. This voltage is then multiplied by an internal calibration factor to yield the particle size information. It should be noted that for light scattering-type aerosol instrument (e.g., LPS), the scattered light is dependent upon instrument properties (optical design, illumination source, etc) and particle properties (size, refractive index, shape, etc). The light scattered by individual spherical particles can be calculated using Mie theory (Hulst, 1981). "And well, we also used the PSL particles before and after the observation experiment. The operation principle of PM monitors has been displayed in the paper which is highlighted in red. The PM monitor (FH62C14) measures the relative humidity immediately upstream of the sample filter-tape assuring a representative measurement of the aerosol conditioning prior to real-time mass determination. So it is no need to worry that the RH affects the measurements.

Question 8: I would suggest to combine fig. 1 and fig. 2 and label the panels as a, b, and c. It is difficult to align low visibility and high RH in separate figures.

Answer: We have specified them in our revised manuscript. The figure shows as below.

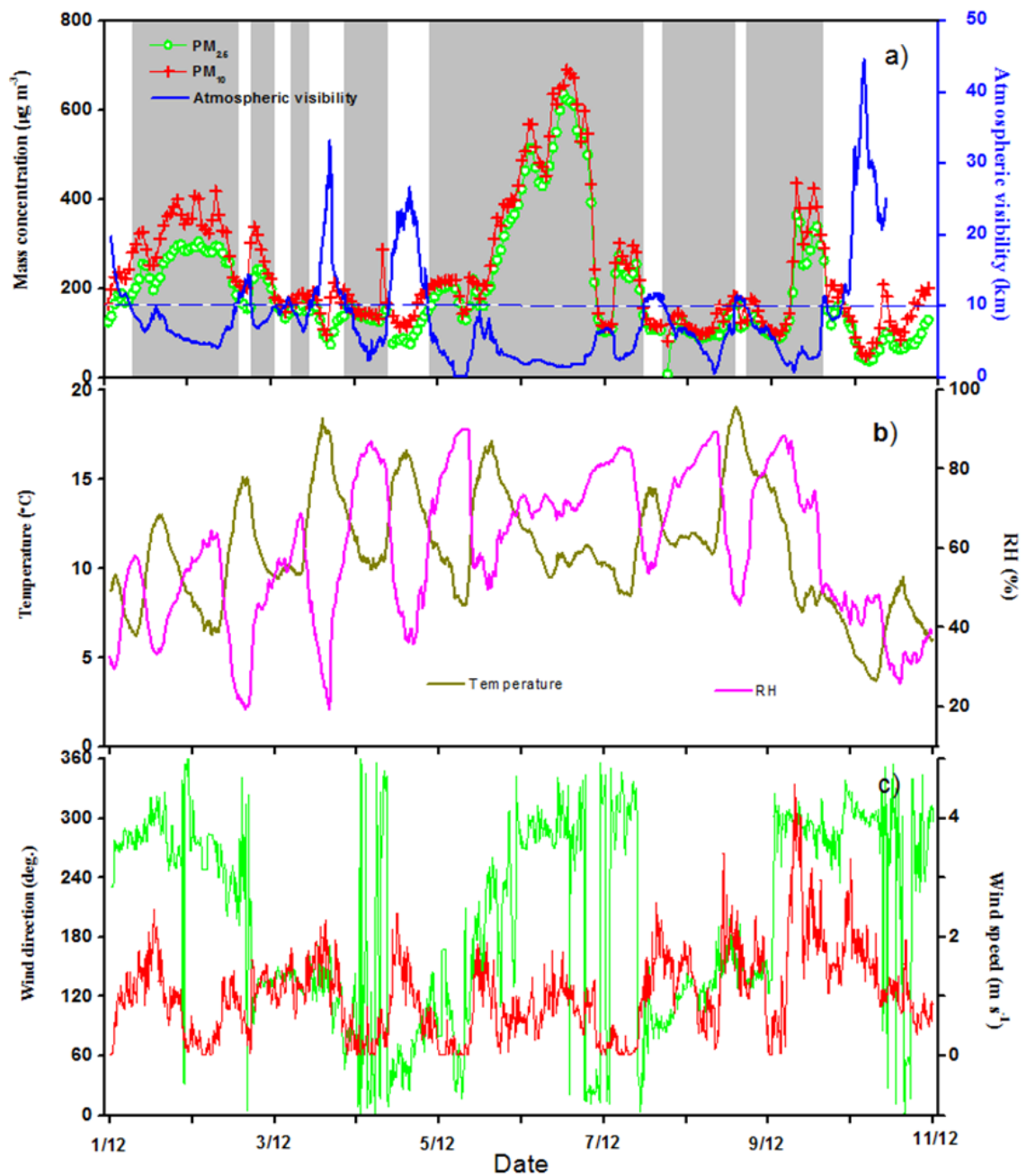


Figure 1. Temporal variations of (a) PM_{2.5}, PM₁₀, atmospheric visibility (Vis) and (b, c) meteorological parameters measured in Shanghai from 1 to 10 December 2013. The dash line is Vis at 10 km.

Question 9: It seems that the record-breaking haze event was regional rather than a local event, because the PM concentrations in other cities in the same region were also high. Consider moving the discussions for AOD maps closer to this paragraph and make this point clearer to readers. When did the PM_{2.5} measurements start in Shanghai? The 600 ug/m³ was a record since when?

Answer: We have moved the discussions for AOD maps (**section 3.2.3**) after this paragraph as **section 3.1.4** and have renewed the order of following sections. We started our measurement using PM monitor at late November, but until the machines were steady and stable, we used the

data of PM. The record 600 ug/m³ was observed during several hours since the midday in 6th Dec.

Question 10: An implicit assumption of the absorption coefficient calculation is that an averaged mixing state of black carbon was used. This should be discussed. Specify the wavelength of data reported. (532 nm?) Also include the single-scattering albedo (SSA) in the analysis?

Answer: An implicit assumption of the absorption coefficient calculation is that an averaged mixing state of black carbon was used. These explain and the wavelength have been added in new **section 3.1.5**. We also added SSA in the new manuscript.

Question 11: P32575, L14 "suggesting that atmospheric oxidation of NO₂ and SO₂ contributed significantly to the formation of nitrate and sulfate". This sentence is confusing. Shouldn't nitrate and sulfate be entirely contributed by NO₂ and SO₂, respectively? Did the authors mean "suggesting that atmospheric oxidation of NO₂ and SO₂ contributed significantly to the formation of particulate matter"? The authors used nitrate/sulfate ratio to discuss contribution of motor vehicles. Nitrate concentration should also depend on the acidity. Abundance of ammonia can play a key role. As suggested in my previous comment, the inorganic species data should be analyzed in a more sensible way by analyzing ion balance or using a thermodynamic model.

Answer: We have specified them in new **section 3.1.7** in our revised manuscript.

Question 12: Include citations for the original data source of weather charts in Fig. 8 and 9. (KMA?)

Answer: We obtained the weather charts (Fig. 8 and 9) from the products of Regional atmospheric and oceanic short-term real-time forecasting system 9.0. One part of this system put the data of Korea meteorological Administration (KMA) on this system to analysis surface weather. We have also corrected the mistake "clod" into "cold".

Question 13: Would the mass concentration calculated by integration of size distribution consistent with measured PM_{2.5} and PM₁₀? Consider the difference between aerodynamic diameter and mobility diameter in the calculation. This kind of closure calculation can be useful for validating data quality. "...no significant correlation was derived between atmospheric visibility and aerosol size of 10–600nm and 1.4–10 μm ". What does this sentence mean? Were the number concentration used in the regressions?

Answer: Before we started our monitor, the WPS had been calibrated according the user manual carefully. We also have compared with other teams to control the data's precision and validity. In new **section 3.2.5**, this sentence we wanted to say that the aerosols in these bins (10–600nm and 1.4–10 μm) have no significant correlations with visibility. Only those aerosols within the diameter interval from 0.6 to 1.4 μm show the expected reciprocal relationship. And the number concentrations used in the regressions display a normal distribution.

Question 14-16: in Figures, Please use discernible colors other than red and pink.

Answer: We have specified them in new figures in our revised manuscript. The figures show as below.

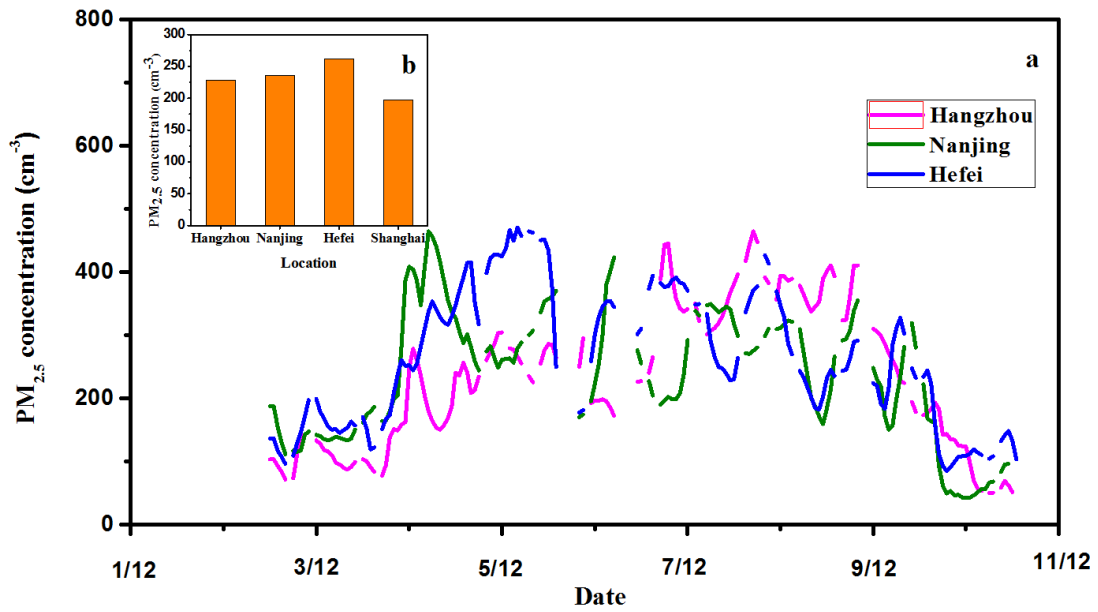


Figure 2. Temporal variations of PM_{2.5} in Hangzhou, Nanjing and Hefei (a) and their mean concentrations (b) from 1 to 10 December.

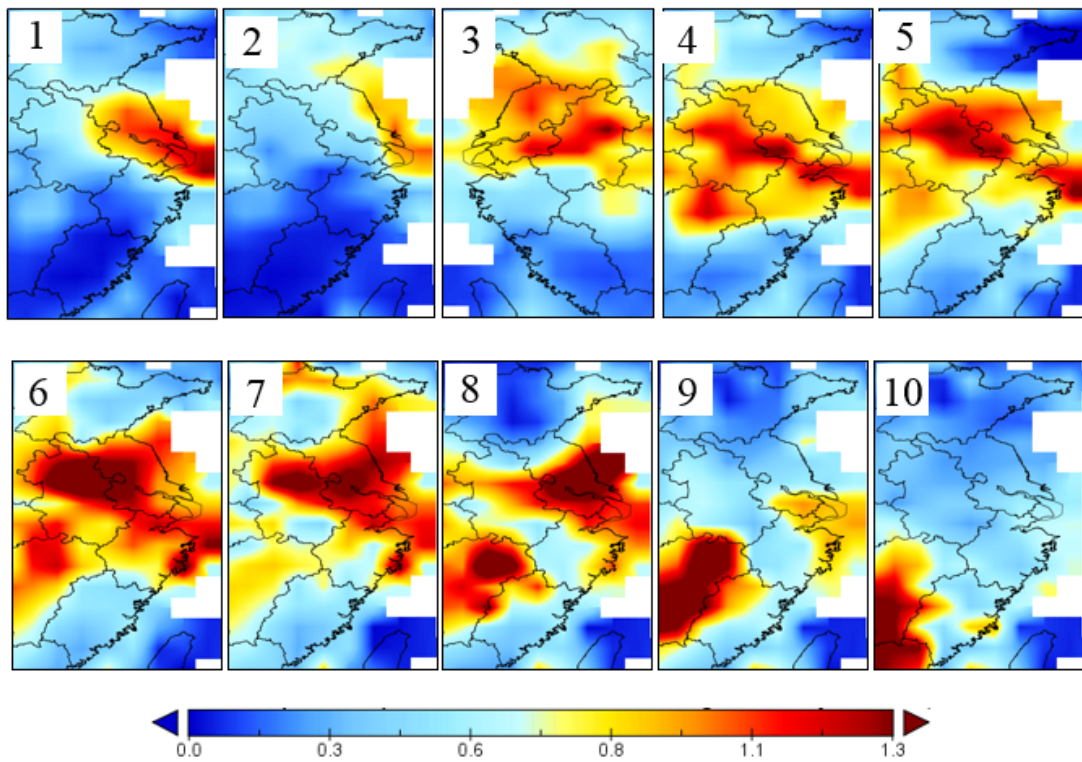


Figure 3. Aerosol optical depth (AOD) at 550 nm from MODIS over the YRD region at 6:00 (UTC) from 1 to 10 December (<http://modis.gsfc.nasa.gov/>).

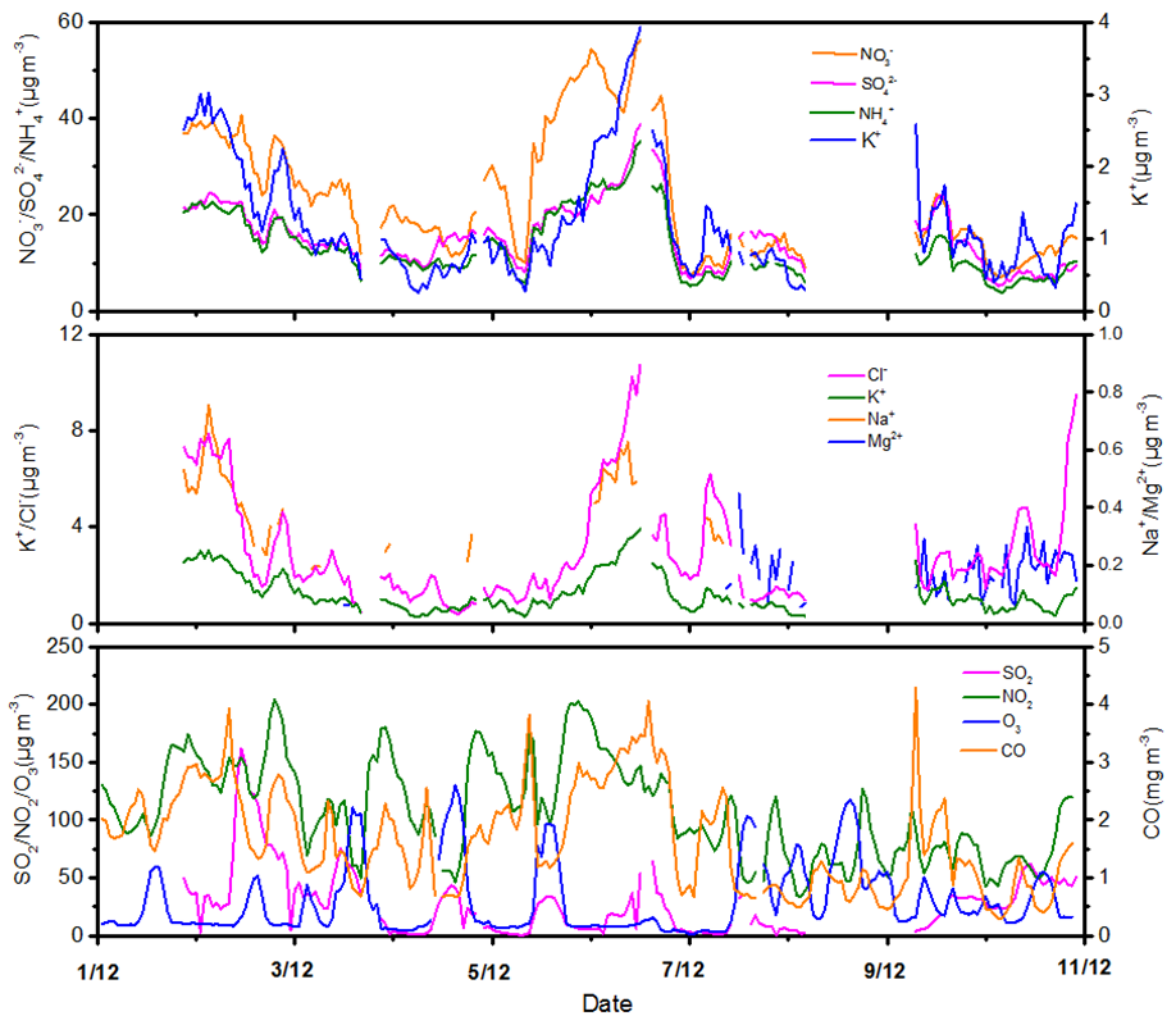


Figure 7: Temporal variations of chemical species in particles from 1 to 10 December.

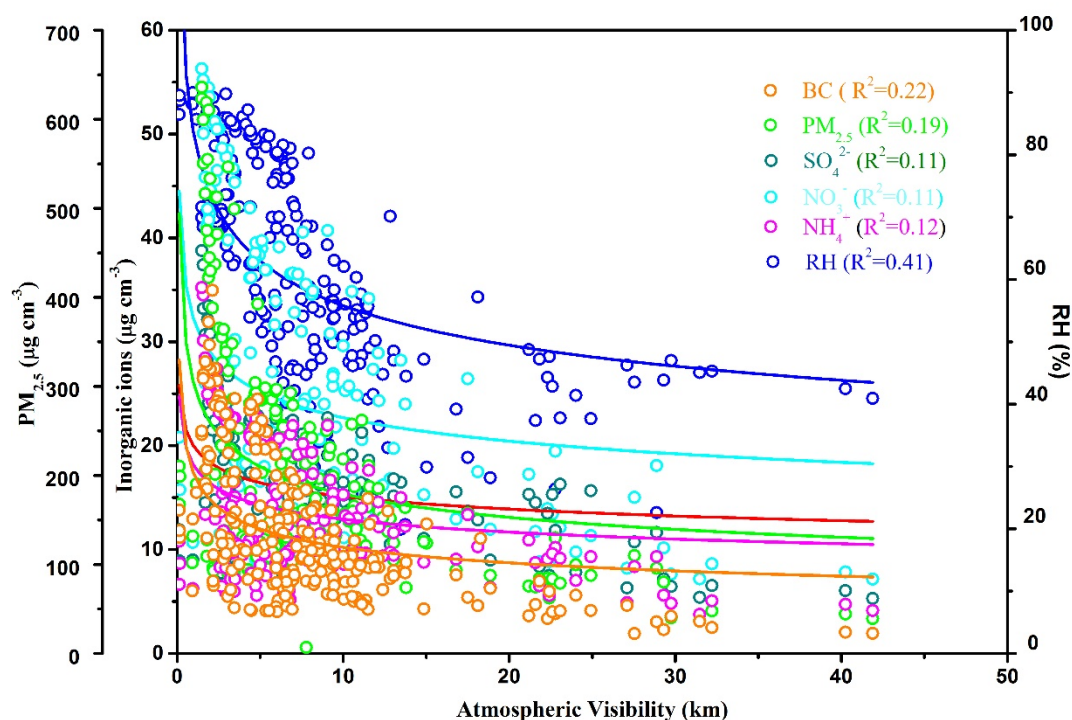


Figure 12: Scatter plots of RH, BC, PM_{2.5} and inorganic ions in particles versus atmospheric visibility.

For Referee 2

Question 1: In the abstract, Correlation between visibility and water soluble ion. Looking at the **Fig. 13** it is difficult to judge whether the low correlation is outcome to selection of wrong function to fit? If that is not the case authors may explain in manuscript.

Answer: In the section which tells the correlation between visibility and water soluble ions, it's not linear relationship between two individual parameters. According to a preliminary analysis of these data, we choose to run nonlinear regression correlation analysis and the fitted curves can be obtained through using the exponential function: $y = ax^b$. We just wanted to study if the single water-soluble ions, not only high ambient RH in large, can directly influence the atmospheric visibility to some extent.

Question 2-8, 13, 21:

Answer: We have specified them respectively using highlight of red in our revised manuscript. And the corrected parts are shown in line 54, 66, 73, 159, 161, 166, 171, 175~185, 270~273, 290 in our new manuscript.

Question 9: In section 2.2, as in previous comment, He et al. (2006) have not discussed errors of overlap correction instead they have cited Welton et al. (2002). Moreover the overlap error is instrument specific and the value 10% reported by Welton et al. (2002) may or may not applicable to system used in this study. Authors should provide their own analysis of error though they may use approach taken by Welton et al. (2002) for determining the error.

Answer: Although we are not discuss errors of overlap correction, but in practice it has been

calibrated in this approach taken by Welton et al. (Welton E.J., Voss K.J., Quinn P. K., Flatau P. J., Markowicz K., Campbell J. R., Spinhirne J.D., Gordon H.R., Johnson, J. E., Measurements of aerosol vertical profiles and optical properties during INDOEX 1999 using micropulse lidars, *J. Journal of Geophysical Research: Atmospheres*, 107, doi: 10.1029/2000JD000038, 2002).

Question 10: In section 2.2: What method was used to control relative humidity in nephelometer. If it was using heated inlet it will reduce volatile and semi-volatile aerosols.

Answer: In order to control relative humidity below 60%, our lab choose to use a silica gel type diffusion drier before the ambient aerosol entering nephelometer. The temperature inside the drier keeps pace with ambient atmosphere. Therefore, it's no need to worry the reduction of volatile and semi-volatile aerosols by using heated inlet instead.

Question 11: In section 2.2: Since the visibility data are discussed in more details later on it will be appropriate if authors provide more details on visibility measurements like what type of sensor was used, what was accuracy and if there were specific data filtering, analysis etc. applied to visibility measurements?

Answer: The Visibility sensor (Belford, M6000) is an instrument used to measure the visibility with a compact, high performance. Visibility is detected using widely accepted principles of forward scattering. A high output infrared LED transmitter projects light into a sample volume, and light scattered in a forward direction is collected by the receiver. The light source is modulated to provide excellent rejection of background noise and natural variations in background light intensity. The absolute accuracy of the Belford Instrument Model 6000 is a result of the accuracy of Belford visibility calibration standards. According to the visibility range (20 ft. to 50 miles), the accuracy of the instrument is 10 ft. ($\pm 10\%$). The data of the instrument was measured at 5 minutes time resolution. Moreover, periodically inspecting the sensor for dirt or other obstructions and carefully cleaning the protective glass windows in the Receiver and Transmitter is particularly necessary for valid measurements. We have added this description in section 2.2 in our revised manuscript.

Question 12: It is authors' assumption that severe haze event might have caused health problem. Either authors should state it as assumption or cite study that has assessed impact of haze on health.

Answer: We have put our citations which had assessed impact of haze on health into our manuscript. Cao et al. (Cao J, Xu H, Xu Q, et al. Fine particulate matter constituents and cardiopulmonary mortality in a heavily polluted Chinese city, *J. Environmental health perspectives*, 120, 373-378, 2012) observed that PM_{2.5} contained with the combustion of fossil fuel had great possibility of an appreciable influence on the health effects in Xi'an.

Question 14: **In section 3.1.5:** Were BC concentration or absorption coefficient estimates corrected for shadowing effect?

Answer: The attenuation cross-sections of other substances like hematite and certain organics such as aromatics rise significantly with decreasing wavelength in the near ultraviolet or even in the visible region. This fact is why most soil and rural airborne dust samples have a brownish color. The presence of strong UV absorption is an indicator for the presence of Fe₂O₃ or some organic compounds (Weingartner et al., 2003, Absorption of light by soot particles: determination of the absorption coefficient by means of aethalometers, *Journal of Aerosol Science*, 34, 1445-1463). Other sources of uncertainty in BC mass concentrations using an Aethalometer arise from instrumental noise, flow rate, filter spot area and detector response. Taking into account all

these effects and the variations in attenuation cross-sections, the overall uncertainty in the reported BC mass concentrations is estimated to be within $\pm 10\%$. Black carbon measured using optical absorption method is often equated to EC in terms of the physicochemical properties such as thermal stability and high light absorption. However, it is possible for some organic components of the ambient aerosol to contribute to the absorptivity of the PM. Adsorption coefficients have been observed to be different on various locations and for different chemical physical mixture of aerosols (Jeong et al., 2004, Measurement of real-time PM_{2.5} mass, sulfate, and carbonaceous aerosols at the multiple monitoring sites, Atmospheric Environment, 38, 5247-5256). Before the campaign of our studies, the attenuation cross section used in the Aethalometer was adjusted to get the greatest accuracy required for site using the method of the comparison between the Aethalometer BC data and the thermal optical analysis EC data described in detail by our other article (Cheng et al. 2010). We have corrected the raw data as far as possible, including shadowing effect.

Question 15: **In section 3.1.5:** Value of alpha (mass absorption efficiency) turns out to be $8.28\text{m}^2/\text{g}$ for 6th Dec. but $7\text{m}^2/\text{g}$ for clean period based on the values provided in the brackets.

Answer: We adopt BC absorption efficiency as $8.28\text{ m}^2/\text{g}$ to calculate aerosol light absorption coefficient with every values. As it illustrates above, this period of time is classified into haze and clear days. The following analysis show the average values of Ab in the clean periods, which were calculated with BC before. In our opinions, we think it's no need to calculate backward using the mean values.

Question 16: **In section 3.1.5:** Absorption coefficient, scattering coefficient and extinction coefficients are function of wavelengths. At what wavelength extinction coefficient was calculated?

Answer: As it's mentioned above in section 2.2 "Aerosol scattering coefficients (525 nm) were measured using an Aurora-1000 nephelometer (Ecotech Pty Ltd., Australia) at 5 min resolution", the three coefficients are all calculated at 525 nm wavelength.

Question 17: **In section 3.1.6:** Authors attribute two peaks in diurnal pattern of number concentration to rush hour traffic. 7th December was Sunday. (Assuming Sunday is holiday in Shanghai) Why is 7th December peaks are not any different from previous days (in fact they are higher than later days) if these peaks are due to rush hour? In fact the statement is contradictory statement to your discussion about effect of boundary layer dynamics on concentration.

Answer: Although Sunday is holiday in Shanghai, there are still rush hours of traffic and two peak pattern because of a very large amount of vehicles and motors (more than 3 millions). Other factors, such as meteorological conditions, e.g. low wind speed and high RH, contribute to pollutant pooling because of bad atmospheric diffusion. On weekend (7th Dec.), higher ambient RH, lower temperature and lower wind speed resulted in low boundary layer and relatively stable nature. We discussed the influence of meteorological factors and RH on pollution formation in the follow sections.

Question 18: **In section 3.1.6:** Authors state that number size distribution is wide during hazy episodes. Authors may consider including analysis on whether this observation consistent with hygroscopic growth of the particles.

Answer: We make great efforts to obtain the number size distribution of particles. To avoid that particles packed with water by the property of hygroscopic growth were detected as bigger improperly, the silica gel diffusion drier was installed before almost every instruments

controlling the relative humidity of ambient aerosol. So we can simply believe that the machines monitor the real sizes of dry particles.

Question 19: **In section 3.1.6:** In discussion of CCN, authors may consider discussing what fraction of N is CCN and whether that fraction changes between hazy and clear days?

Answer: For the important role of CCN in the population of atmospheric aerosol, we must understand the source, properties, impact factors and their evolution. So we paid great attention on discussing what fraction of condensation nuclei is CCN and whether that fraction changes between hazy and clear days.

Question 20: **In section 3.1.7:** conclusion drawn in this section about vehicular vs stationary sources based on ratio of nitrate to sulphate ion is not included in conclusion section as well as in abstract!

Answer: we have already added the conclusion in conclusion section and in abstract in highlight.

Question 22: **In section 3.2.4:** Authors state that during Haze (which is also a period of high pollution) kappa values are high but during clear day kappa values are low. Also the kappa value reported in this study are substantially lower than values reported for Beijing by Gunthe et al. (2011).

Answer: We have downloaded and carefully read the paper you supplied. Both of us reported the effective hygroscopicity parameters (κ), and noticed that the parameter can be calculated as a function based organic and inorganic mass fractions (f_{org} , f_{inorg}). Gunthe et al. (2011) reported decrease in kappa value with increase in pollution, it is really contrast to our result. But Kappa is calculated along with the data of chemical compositions. When larger proportion of mass fractions during the pollution is organic compounds, it will meet smaller values of Kappa. The parameter does not directly related to the occurrence of pollution. That is to say the hygroscopicity parameter (kappa) depends on chemical compositions and their amounts.

Question 23: **In section 3.2.4:**For a correlation analysis to be useful, authors should report more details on how did they arrived on choice of functions for fitting, what were significance test done?

Answer: The similar answer can be found in question 1.

Question 24: **Fig. 1:** In spite of low PM_{2.5} and PM₁₀ on 8th December (and 4th Dec. morning) visibility is low. Authors may elaborate on it in the manuscript.

Answer: Based on the general meteorological conditions (e.g., wind speed, wind direction, RH and temperature) on 8th Dec. and 4th Dec. morning, higher ambient RH, lower temperature and lower wind speed may determine the phenomenon of this kind. Even the concentrations of PM_{2.5} and PM₁₀ were low, we have one part to analysis the potential contribution of BC and ambient RH to atmospheric visibility impairment. According to the result, it is reasonable to some extent that low PM_{2.5} and PM₁₀ exist with the low visibility. We have added more manuscript about it.

Question 25: **Fig. 7:** CO concentration in range of 1 to 3 $\mu\text{g}/\text{m}^3$ are extremely low values. For example Gao et al. (2005) have reported CO values of the order of several hundred $\mu\text{g}/\text{m}^3$ at Mt. Tai. I expect CO concentration in Shanghai higher than Mt. Tai.

Answer: We have specified them in new figure 7 in our revised manuscript. The figure shows as below.

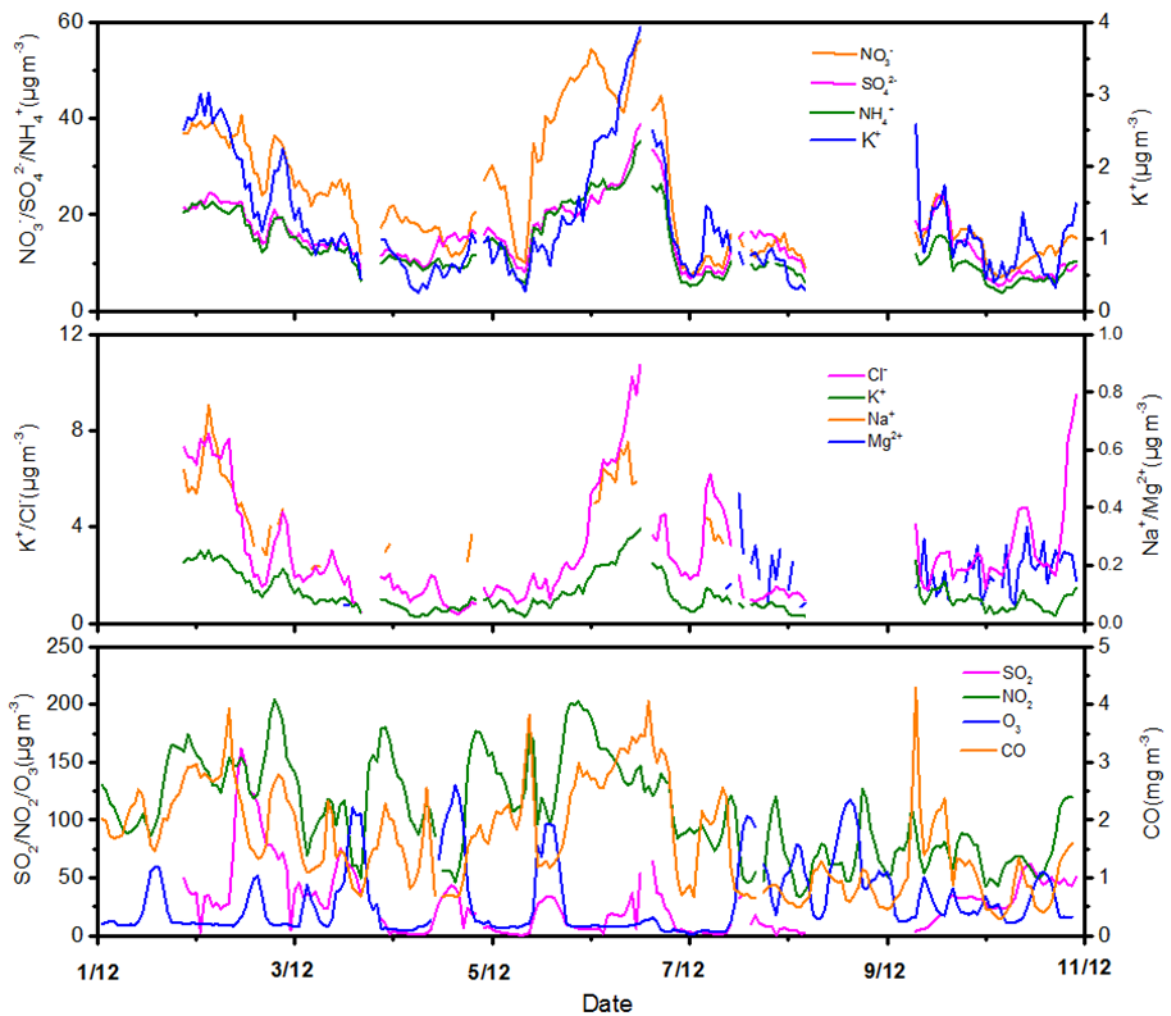


Figure 7: Temporal variations of chemical species in particles from 1 to 10 December.

Technical Comments

Question 1-3, 5-6 and 8-10

Answer: We have read the manuscript very carefully and corrected any places having grammar errors or mistakes, which are highlighted in red in the revised manuscript.

Question 4: Page 32565 Line 18: "... Shanghai based on online water ..." What is meaning of online here?

Answer: We use MARGA to monitor aerosol and gases at 1h time resolution, which may much higher than other chemical analyzers. So, the meaning of online can be likely to be expressed as synchronous or simultaneous.

Question 7: Page 32573 Line 2: What is meaning of word "integrating" here. Appears to me confusing along with word "size-resolved" used in the same sentence.

Answer: We use the instrument WPS-1000 XP to obtain a time series of aerosol size spectra. It separates polydisperse aerosol particles by size for high-resolution measurements of particle-size distribution. So, I mean the word "size-resolved" here equals to "particle-size distribution", and the word "integrating" equals to "having integrals by using number concentrations of particle-size distribution".

For Referee 3

Question 1: The manuscript would clearly gain in strength if edited by native English speaker. Currently, it contains too many grammatical errors and some sentences are difficult to follow.

Answer: We have read the manuscript very carefully and corrected any places having grammar errors or mistakes, which are highlighted in red in our revised manuscript. And the manuscript have been revised partly by one native English speaker.

Question 2: My reading of that this manuscript presents many raw data, with finally little interpretation. So maybe the authors could decide to present extensively all data providing ground for further investigations (in another study) of the specific features of that event i.e., with little or no data treatment. They could also select to present here the real specificities of that event. I feel that the current version oscillates between both options, which weakens the associated message.

Answer: As you mentioned, this manuscript presents many raw data. Aerosol physical, chemical and optical properties were measured and examined to give insights into severe haze events in the YRD. We mainly put efforts to combine ground base observations with views of synoptic during the entire process of haze pollutions. So, we guess that it would be meaningful to investigate the formation and evolution of regional haze events, and to support useful information for pollution forecast and how to reduce the incidence of regional atmospheric pollutions. It's really important to throw light on more specific features of that event, much deeper research and investigations will be contained in our another study of this haze event.

Question 3: One of the clearly strong aspect of that investigation, is the quite large number of parameters that have been reported, but finally not really used.

Answer: We used various data to draw a whole picture of this severe haze event. The first aim is to analyze the situation of entire pollution including pollutant, meteorological etc. The second aim is to analyze the formation of pollution event. Therefore, we need make more analysis for the pollution based on so rich data. We have given deeper analysis In the new manuscript.

Thanks very much!

2016-6-12

Insights into a historic severe **haze event in Shanghai:
synoptic situation, boundary layer and pollutants**

Chunpeng Leng ^a, Junyan Duan ^a, Chen Xu ^a, Hefeng Zhang ^b, Yifan Wang ^a, Yanyu Wang ^a, Xiang Li ^{a*}, Lingdong Kong ^a, Jun Tao ^c, Renjian Zhang ^d, Tiantao Cheng ^{a,e*}, Shuping Zha ^e, Xingna Yu ^e

- a. Shanghai Key Laboratory of Atmospheric Particle Pollution and Prevention (LAP³), Department of environmental science and engineering, Fudan University, Shanghai 200433, China;
- b. Atmospheric Environment Institute, Chinese Research Academy of Environmental Sciences, Beijing 100012, China;
- c. South China Institute of Environmental Sciences, Ministry of Environmental Protection, Guangzhou 510655, China;
- d. Key Laboratory of Region Climate-Environment Research for Temperate East Asia, Institute of Atmospheric Physics, Chinese Academy of Sciences, Beijing 100029, China;
- e. Key Laboratory of Meteorological Disaster of Ministry of Education, Nanjing University of Information Science and Technology, Nanjing 210044, China;

* Corresponding authors: Tiantao Cheng, Xiang Li

Tel: (86) 21-6564 3230; fax: (86) 21-6564 2080;

Email: ttcheng@fudan.edu.cn, lixiang@fudan.edu.cn

Abstract

A historic **haze event**, characterized by long duration, large scale and **severe** pollution, occurred in the Yangtze River Delta (YRD) of China during 1 to 10 December 2013. **This haze event** significantly influenced air quality throughout the region, especially in urban areas. Aerosol physical, chemical and optical properties were measured in Shanghai. **Sometimes** the instantaneous particle concentration (e.g. $\text{PM}_{2.5}$) exceeded $600 \mu\text{g m}^{-3}$. Inorganic water-soluble ions in particles, trace gases and aerosol optical coefficients had **a similar** tendency to increase evidently from clear to hazy episodes. A combination of various factors contributed to the formation and evolution of the haze event, among which meteorological conditions, local anthropogenic emissions and **pollutants** are the major factors. **High pressure system, calm surface wind and subsidence airflow were responsible for the decrease of planetary boundary layer (PBL) and the accumulation of pollutants. Atmospheric visibility correlated strongly with relative humidity (RH), particle number in size of 600-1400 nm other than particulate water-soluble species and particle mass ($\text{PM}_{2.5}$). The particle hygroscopicity plays an important role in atmospheric visibility reduction. The results are somewhat helpful to forecast and eliminate regional atmospheric pollutions in China.**

Key words: haze, air pollution, formation mechanism, urban

1. Introduction

Atmospheric aerosols are either emitted from human activities and natural sources or formed by a variety of precursor photochemical reactions. Aerosol exerts great impacts on the earth's radiation balance and climate by directly scattering and absorbing solar and terrestrial **radiation**, and indirectly modifying cloud and **precipitation** by acting as cloud condensation nuclei (CCN) (Ramanathan et al., 2001; Andreae et al., 2005; Lohmann et al., 2005). In **lower atmospheric layers**, aerosol particles can **accumulate** and result in air pollutions under unfavorable **dispersion conditions**, and then produce the adverse effects on human health and atmospheric visibility (Wu et al., 2005). Haze is an atmospheric phenomenon that the sky clarity is obscured by dust, smoke and other dry particles, during which atmospheric visibility and relative humidity (RH) are usually below 10 km and 80% (Wu et al., 2006; Xiao et al., 2006; Fu et al., 2008; Bell et al., 2011).

Since World War II, haze has occurred in London and Los Angeles due to fast economic development (McNulty, 1968; Lee, 1983; Schichtel et al., 2001). After that, the regions affected by haze have **spread to North Africa, Indian Ocean and Asia etc.** (Quin and Bates, 2003; Huebert et al., 2003; Du et al., 2011). Until now, the formation and evolution of haze has not been fully understood despite of experiments carried out throughout the world, making it difficult for the governments to take effective

measures to reduce air pollutions (Malm and Day, 2001; Huebert et al., 2003; Wu et al., 2005; Wang et al., 2006b).

China has undergone rapid economic and social development for over 30 years, which releases a large amount of anthropogenic particles and relevant precursors, and forces many cities to suffer from atmospheric pollutions. The increase of haze or hazy days have been observed in the urban environments of northern, eastern, and southwestern China (Sun et al., 2006; Che et al., 2009). Four major regions are mostly influenced by haze in China, i.e. the Jing-Jin-Tang Region (JJT), the Yangtze River Delta (YRD), the Sichuan Base (SCB) and the Pearl River Delta (PRD). The hazy days increased significantly from 70d in 2001 to 144d in 2004 in Guangzhou (Liu et al., 2013). Although the hazy days decreased quickly from 223d in 1982 to 73d in 2005 in Beijing after measures implemented on management of coal demand, motor vehicles, industrial and dust emissions, however, it increased again in 2011 and posed significant effects on human society (Liu et al., 2013). Wang et al. (2006b) compared the aerosol chemical compositions of dusty, hazy and clear days in Beijing, and pointed out that $(\text{NH}_4)_2\text{SO}_4$, NH_4NO_3 and $\text{Ca}(\text{NO}_3)_2$ were the major species during hazy days in spring. Sun et al. (2006) found that the concentrations of aerosol elements and water-soluble ions in haze-fog episodes were over 10 times those in clear days in Beijing. The YRD region, one of important economic core areas with large population, high

urbanization and advanced industrialization in China, is facing an **inter-annual** increase of foggy and hazy days, especially in winter (Tie and Cao, 2009). Ye et al. (2011) discovered the important role of ammonia in haze formation in Shanghai. Du et al. (2011) put insights into summer **haze events** over Shanghai, and pointed out that the secondary pollutants of increasing sulfate and nitrate were oxidized from large amounts of SO₂ and NO₂ under a high atmospheric oxidation condition. Kang et al. (2013) regarded more accumulation mode particles and higher RH as the main reasons of atmospheric visibility impairment during haze episodes in Nanjing.

To date, available studies on haze in the YRD mainly put efforts to the chemical compositions and physical characteristics of pollutants, but in view of synoptic few focused on the entire process of **events at larger scales**. It is meaningful to investigate the formation and evolution of regional **haze events** for useful information to forecast and reduce severe atmospheric pollutions. A winter haze event occurred in the YRD during 1-10 December 2013, known as one historic severe **event** with features of long duration, large scale and strong pollution. This paper performs a detailed analysis of this serious **haze event** and gives insights into regional heavy atmospheric pollution in such a fast-developing area.

2. Experiment

2.1 Observation site

The measurement station was mounted on the roof of one building approximately 20m above ground in the campus of Fudan University (31°18'N, 121°29'E) in Shanghai, located in the east edge of the YRD region. The site is mainly surrounded by urban residential and commercial zones, approximate 40 km from the East China Sea. **Due to Asian monsoon climate, the annual mean precipitation is about 1119 mm**, mainly occurring between May and September, and the wind prevails northeasterly in winter and southeasterly in summer. **Atmospheric components are likely to originate** from local emissions and remote sources (Du et al., 2011). Local time (LT) used in this study is eight hours ahead of UTC.

2.2 Instrument and Measurements

Major water-soluble ions (Na^+ , K^+ , Mg^+ , Ca^+ , SO_4^{2-} , Cl^- , NO_3^- and NH_4^+) in aerosol particles were measured by an analyzer for Monitoring Aerosols and Gases (MARGA, ADI 2080, Netherlands) at 1 h time resolution. Ambient air is drawn into the sample box with airflow of $1 \text{ m}^3/\text{h}$ by **a pump with mass** flow controller (MFC), and the **separated gases and aerosols are selectively dissolved and then analyzed by ion chromatography**. An internal calibration method, using bromide for the anion chromatograph and lithium for the cation chromatograph, was operated over the whole period to ensure the instrument to identify and measure ion species successfully. The detailed information of **sampling**,

operation and internal calibration can be found elsewhere (Du et al., 2011).

Aerosol particle size distributions in 10nm - 10 μ m were observed using a high-resolution wide-range particle spectrometer (WPS-1000 XP, MSP). The principle of instrument, combining laser light scattering (LPS), condensation particle counting (CPC) and differential mobility analysis (DMA), has been introduced in detail by Gao et al. (2009). DMA and CPC can effectively count particles in 10nm - 500nm, while LPS is designed to measure particles in 350nm - 10 μ m. The instrument took 3 min to scan the entire size range completely, 60 channels in DMA and 24 channels in LPS (2 s per channel). Before the campaign, DMA was calibrated using the National Institute of Standards and Technology (NIST) Standard Reference Materials (SRM) 1691 and SRM 1963 Polystyrene Latex (PSL) spheres (mean diameter of 0.269 μ m and 0.1007 μ m) to maintain **transfer function** proper and accurate particle sizing. LPS was calibrated using four NIST traceable sizes of PSL (i.e. 0.701, 1.36, 1.6 and 4.0 μ m). Zhang et al. (2010) has described the calibration and operation methodology of WPS in detail.

Black carbon (BC) was measured by an Aethalometer (AE-31, Magee Scientific Co., USA) at 5-min time resolution and 5 l/min airflow rate. According to the strong ability of BC absorption to near-infrared lights, its mass can be determined using the light attenuation at 880 nm and the appropriate specific attenuation cross section proportional to BC (Petzold et al., 1997). The attenuation is calculated based on the intensity difference

of reference and sensing beams between light on and off (Hansen et al., 1984; Weingartner et al., 2003). In order to screen the impacts of other absorptive material, the data contaminated by mineral ~~and dust~~ aerosols were excluded from BC measurements. Details for instrument operating and calibrating and **data processing** can be found in Cheng et al. (2010).

Aerosol backscattering profile was measured by a set of micro pulse lidar (MPL-4B) with pulse energy 6-10 μ J and repetition frequency 2500 Hz. To date, MPL is utilized widely in the **most parts of world** as an effective tool for capturing high temporal resolution information of aerosol vertical distributions (Menut et al., 1999; Cohn and Angevine, 2000; Brooks, 2003). Planetary boundary layer (PBL) height is determined by the MPL measurement at the altitude where a sudden decrease of scattering coefficients occurs (Boers and Eloranta, 1986). **Instrument calibrations, normalization process, and the analyses of errors propagation and correction uncertainties in MPL processed signal have been described by Campbell et al. (2002), Welton and Campbell (2000) and Welton (2002).** ~~To avoid underestimation of aerosol scattering at the lowest altitudes with the majority of aerosol population, the overlap issue is concerned and solved experimentally (Campbell et al., 2002). In general, MPL is set horizontally to obtain an averaged atmospheric data in the late afternoon~~ **without obscuration attribute to relatively lower aerosol loading and well mixed atmosphere**, under which condition the backscattering in the target

layer is roughly assumed to constant. The calibrations operated in 2009 showed that the full overlap is about 4 km, and the raw data need to be corrected by the overlap correction function (He et al., 2006). The uncertainty induced by the overlap correction has been fully discussed and estimated to be less than 10% (Welton et al., 2002; He et al., 2006).

Aerosol scattering coefficients (525 nm) were measured using an Aurora-1000 nephelometer (Ecotech Pty Ltd., Australia) at 5-min resolution. The scattering coefficient is calculated by integrating the scattering intensities from angles 7° to 170°. The relative humidity (RH) inside the instrument was retained below 60% to prevent from excessive water vapor entering the chamber. The zero check was operated automatically each day using particle-free air, while the span check was done every two weeks using R-134a gas.

A CCN counter (CCN-100, DMT, USA) with continuous flow and single column (Roberts and Nenes, 2006; Lance et al., 2006) was employed to monitor CCN concentrations at supersaturations (SS) of 0.2-1.0%. The ambient aerosols were firstly dried by a dryer (activated carbon) to lower relative humidity (RH) below 30%, and subsequently introduced into the counter. The instrument was calibrated for SS using standard $(\text{NH}_4)_2\text{SO}_4$ particles every three months since 2010. According to the instrument operation manual, regular calibrations were also performed for temperature gradient, input and shear airflows and pressure to maintain stable SS (Leng

et al., 2013, 2014a, b). Periodic zero checks were done to ensure counting accuracy for optical particle counter (OPC) inside the CCN counter.

Moreover, two continuous ambient particulate monitors (FH62C14, Thermo) were used to measure PM_{2.5} and PM₁₀ (particles in aerodynamic diameter <2.5 μm and <10 μm). **The particles are deposited on a glass fiber tape, and then detected by the method of beta attenuation. The particle mass concentration is obtained from the simultaneous measurements of mass and volume of one aerosol sample.** An automatic weather station (HydroMet, Vaisala) and a visibility monitor (Vaisala) were employed to measure meteorological variables and atmospheric visibility. The data of hourly-averaged conc. of gases (SO₂, NO₂, CO and O₃) was from the Shanghai Environmental Monitoring Center (SEMC).

3. Results and discussion

3.1 Overview of haze event

3.1.1 Identification of hazy episode

It has been widely accepted that the key criterion for discerning a **haze event** is an apparent decrease of atmospheric visibility less than 10 km and ambient relative humidity (RH) below 80% lasting for several hours (Fu et al., 2008; Du et al., 2011). When 80% < RH < 90%, the event is referred to as a complex of haze-fog co-occurring or transition (Leng et al., 2014a), and it is also classified into hazy episode in the present study.

Figure 1a depicts the temporal variations of hourly PM_{2.5}, PM₁₀,

atmospheric visibility and meteorological factors from 1 to 10 December 2013. On the whole, atmospheric visibility mostly declined to below 10 km, and RH hardly reached 90%. The **haze event** constituted of several sub-episodes, marked by gray areas in **Figure 1a**. It was clear that Shanghai suffered from **a long-term haze event** until 10 December, and subsequently loosened when atmospheric visibility improved and the clean sky took control afterwards. In fact, these hazy sub-episodes approximately accounted for 70% of the entire period, with mean atmospheric visibilities of 5.65 km for the former compared to 29.45 km for the rest (30%).

On a larger scale, this **haze event** caused a historic atmospheric pollution, and attacked the most parts of central and eastern China. $\text{PM}_{2.5}$ in many cities exceeded $150 \mu\text{g m}^{-3}$, and some more than $300\text{-}500 \mu\text{g m}^{-3}$ even $600 \mu\text{g m}^{-3}$, **as expected**, this **event** will produce one serious problem to people's health at that time (**Cao et al., 2012**).

3.1.2 Meteorological conditions

Precipitation did not appear during the whole campaign. For most of the period (**Figure 1b and 1c**), ambient RH and temperature correlated negatively and showed an evident diurnal pattern, varying in the ranges of 20-87% and 6-17 °C, respectively. The hazy episodes were usually characterized by higher RH and lower temperature, while the clean periods often corresponded to lower RH and higher temperature. The main reason is that high temperature can strengthen the vertical dispersion of pollutants

due to thermal effects, and high RH can facilitate aerosol scattering due to hygroscopicity. The wind was weak ($< 2 \text{ m s}^{-1}$, 87%) during the hazy episodes until 9 December, but in the following day it became strong ($>4 \text{ m s}^{-1}$) and conducive to the dispersion of air pollutants due to transiting cold front (Figure 1b and 1c). The wind direction was basically northeast or southeast during the clean periods, originating from marine areas. However, the wind normally turned into northwest when the haze took over, which will probably bring a large quantity of pollutants from inland areas and to some extent cause pollutant accumulation in downwind.

3.1.3 Particulate mass concentration

PM_{2.5} and PM₁₀ were employed to represent ambient particulate mass burden per volume in the atmospheric boundary layer. PM_{2.5} and PM₁₀ instantaneously ranged within 50-600 $\mu\text{g m}^{-3}$ and 55-680 $\mu\text{g m}^{-3}$ throughout the whole campaign (Figure 1a), and both of them significantly rose during the hazy episodes with averages of 315 and 333 $\mu\text{g m}^{-3}$, compared to 112 and 134 $\mu\text{g m}^{-3}$ in the clean periods. On the other hand, the ratios of PM_{2.5}/PM₁₀ varied between 0.54 and 0.97, and averaged at 0.88, 0.93, 0.8 in total, hazy and clean periods, indicating that the fine particles are major contributors to particle mass.

Interestingly, both PM_{2.5} and PM₁₀ reached their peaks of 600 and 680 $\mu\text{g m}^{-3}$ as new historic records on 6 December, approximately 14 times higher than the Grade I criteria of the National Ambient Air Quality

Standard of China ($50 \mu\text{g m}^{-3}$ for PM_{10}), and 24 times the World Health Organization Air Quality Guidelines ($25 \mu\text{g m}^{-3}$ for $\text{PM}_{2.5}$). Other cities in the YRD showed a similar tendency and high $\text{PM}_{2.5}$ along with this haze event, such as $226 \mu\text{g m}^{-3}$ in Hangzhou, $230 \mu\text{g m}^{-3}$ in Nanjing and $260 \mu\text{g m}^{-3}$ in Hefei (Figure 2). The numerous measurements earlier in Shanghai during the last decade showed much lower values. For example, Wang et al. (2006a) observed that $\text{PM}_{2.5}$ varied within $17.8\text{-}217.9 \mu\text{g m}^{-3}$ and averaged at $94.6 \mu\text{g m}^{-3}$. According to the Shanghai Environmental Bulletin 2010 (www.envir.gov.cn/law/bulletin/2010/), the annual average of PM_{10} in 2009 was about $79 \mu\text{g m}^{-3}$. Leng et al. (2014a) reported $\text{PM}_{2.5}$ average of $143 \mu\text{g m}^{-3}$ during hazy episode and $46 \mu\text{g m}^{-3}$ during clear episode in November 2010. They also observed that $\text{PM}_{2.5}$ varied in $10\text{-}210 \mu\text{g m}^{-3}$ in January 2011 and $10\text{-}130 \mu\text{g m}^{-3}$ in April 2012, respectively (Leng et al., 2013, 2014b). In addition, compared to Beijing as another megacity in China, He et al. (2001), Sun et al. (2004) and Liu et al. (2013) monitored $\text{PM}_{2.5}$ extremes of $357 \mu\text{g m}^{-3}$ from July 1999 to September 2000, $349 \mu\text{g m}^{-3}$ in winter from 2002 to 2003, and $220 \mu\text{g m}^{-3}$ in September 2011. Briefly, the particulate mass burden was extremely high in this haze event, and so serious air pollution, unsuitable for human beings (Liu et al., 2013), must cause a formidable environmental disaster.

3.1.4 High aerosol columnar loading

Aerosol optical depth (AOD), retrieved from MODIS employing the

algorithm well introduced by Li et al. (2005), can be acted as a good indicator of aerosol loading in the whole atmosphere. Figure 3 depicts a full feature of AOD spatial distribution and its day-to-day development during the haze event. Briefly, the covering region of high AODs (>0.5) was generally spreading out a big domain, about most of the South China. High AODs originated from the YRD and the SCB, then extended to the central South China, the southwestern China and even the south of the JJT region, and moved to the YRD area in the end.

In the most serious days, AODs were as high as 1.00-1.25 on 5-8 December. According to the records of the Ministry of Environmental Protection of China (<http://www.zhb.gov.cn/>), many cities in the upwind areas (e.g. Nanjing, Wuxi, and Suzhou) had higher AODs up to 1.5 and AQI over 500, implying that the inflow of pollutants to Shanghai is inevitable to contribute to the pollution. In addition, the weak circulation (Sect. 3.2.1) normally led to the build-up of pollutant pooling and contributed to the haze event formation.

3.1.5 Aerosol optical properties

Figure 4 shows a temporal series of BC, aerosol scattering coefficient S_c (525 nm), and aerosol absorption coefficient A_b (532 nm). Based on the assumption that the averaged mixing state of BC is uniform, the A_b coefficient is indirectly calculated from measured BC according to the following equation (Yan et al., 2008),

$$A_b = \alpha \times [BC] \quad (1)$$

where [BC] represents BC mass concentration, and α is BC absorption efficiency which is adopted as 8.28 g m^{-2} in this paper. This value was obtained from the inter-comparison experiment performed in southern China previously, and was within the variance range of various source regions (Bergin et al., 2001; Bond and Bergstrom, 2006; Yan et al., 2009; Zhao et al., 2013). The aerosol scattering and absorption coefficients in combination determine its extinction ability, namely aerosol extinction coefficient ($Ex = Ab + Sc$).

Basically, BC, Sc and Ab had the same tendency to increase in the hazy episodes, and reached to their max values at 0:00 LT on 6 December, i.e. $35 \mu\text{g m}^{-3}$, $2.8 \times 10^3 \text{ M m}^{-1}$ and 290 M m^{-1} , approximately 4-5 times higher than their mean values in the clean periods ($8.3 \mu\text{g m}^{-3}$, 643 M m^{-1} and 58 M m^{-1}). The enhancement of aerosol optical properties largely contributed to atmospheric visibility decreasing, which correspondingly deteriorated to its minimum of 50 m at the same moment (Figure 1). **The mean aerosol single scattering albedo ($SSA = Sc/Ex$, 532nm) was expectedly low at 0.89, indicating more absorptive species existing in the particle group.**

3.1.6 Condensation nuclei and cloud condensation nuclei

Aerosol size distribution was analyzed in detail to shed some light on its relationship with haze. Figure 5a presents a time series of aerosol size spectra and integrating particle size-resolved number concentrations (N_{CN}).

N_{CN} showed an evident diurnal pattern with two peaks corresponding to the traffic rush hours, and appeared higher mean and instantaneous values in the hazy episodes (15000 and 25000 cm^{-3}) than the clean periods (9500 and 17000 cm^{-3}). Generally, ambient aerosol particles in higher loading mainly distributed in a wider size range over the hazy episodes than the clean periods, 20-200 nm for the former and 20-100 nm for the latter. The averaged aerosol number size distribution is shown in Figure 5b. About 67% of particles fell in the size range of 10-100 nm, and the percent further increased to 91% when enlarged to 10-200 nm. This result is in good agreement with the early observations that urban ambient aerosols mainly distribute in ultrafine size section (Woo et al., 2001; Gao et al., 2007), slightly higher than 62% reported in Nanjing and 61% in Atlanta, a little lower than 72% in Eastern Germany and significantly lower than 94% in Taicang (Woo et al., 2001; Tuch et al., 1997; Gao et al., 2009; Kang et al., 2013).

Cloud condensation nuclei (CCN) constitutes an important fraction of atmospheric aerosol population, and can indirectly influence global climate change through modifying the microphysical and radiative properties and lifetime of cloud (IPCC, 2013). It tends to reduce cloud droplet size and then suppress the wet precipitation in shallow and short-lived clouds (Lohmann and Feichter, 2005). Previous studies in Shanghai have found that CCN number concentration (N_{CCN}) and aerosol activity promotes

effectively during the polluted periods (Leng et al., 2013, 2014). In north India, Ritesh et al. (2007) observed a significant impact of winter haze on N_{CCN} . To gather more information about CCN during haze, hourly N_{CCN} at SS of 0.2-1.0% were plotted as a function of time in Figure 6. As expected, N_{CCN} increased with SS, i.e. 3800-10000 cm^{-3} at SS 0.2% and 4000-16000 cm^{-3} at SS 1.0%, and exhibited bimodal daily distributions. Agreed well with N_{CN} , N_{CCN} greatly enhanced during the hazy episodes, about 1.6-1.8 folds (on varying SS) of that during the clean periods.

3.1.7 Aerosol chemical species

A key for understanding haze is to characterize both aerosol composition and trace gases quantitatively (Du et al., 2011). As important components of atmospheric particles, water-soluble inorganic ions are thought to be a significant contributor to atmospheric visibility impairment (Kang et al., 2013).

The time series of hourly water-soluble inorganic ions in $PM_{2.5}$, including Na^+ , K^+ , Mg^+ , Ca^+ , SO_4^{2-} , Cl^- , NO_3^- and NH_4^+ , and gaseous pollutants such as SO_2 , NO_2 , CO and O_3 from 1 to 10 December are **presented** in Figure 7. Aerosol water-soluble ions, highly coinciding with particulate mass, showed higher contents in the hazy episodes than the clean periods. Totally, the mean concentrations of these ions were comparable to that monitored earlier in Shanghai (Yao et al., 2002; Wang et al., 2006a; Du et al., 2011). The mean concentrations of these ions were

in sequence of $\text{NO}_3^- > \text{SO}_4^{2-} > \text{NH}_4^+ > \text{Cl}^- > \text{K}^+ > \text{Na}^+ > \text{Mg}^{2+}$, and their contributions to $\text{PM}_{2.5}$ were 11.7%, 7.7%, 6.7%, 1.5%, 0.6%, 0.3% and 0.08%, respectively, slightly higher than that observed in haze pollutions in Nanjing and Guangzhou (Tan et al., 2009; Kang et al., 2013). Overall, the integrated water-soluble ions accounted for 28.5% of $\text{PM}_{2.5}$, higher than the dust event but significantly lower than the biomass burning event observed in Nanjing (Zhang et al., 2012).

Gaseous species play a vital role in atmospheric process by acting as precursors or mediums of photochemical reactions. Among them, O_3 has been widely known as the products of photochemical reactions between volatile organic compounds (VOCs) and nitrogen oxides (NO_x) with the participation of heat and sunlight, while SO_2 , NO_2 , and CO are mainly emitted from biomass, fuel and coal burning (Seinfeld and Pandis, 2006). Seen in Figure 7, the measured gaseous pollutants behaved an increasing trend during the hazy episodes, with one exception of O_3 probably due to consumption by oxidation of NO and other species (Liu et al., 2013).

NO_3^- and SO_4^{2-} are products of NO_2 and SO_2 due to atmospheric oxidation, hence their concentrations strongly depended on related gaseous precursors and oxidation rate in the atmosphere. Two equations are used to estimate the extent of this transformation process (Sun et al., 2006):

$$\text{NOR} = \frac{n\text{NO}_3^-}{(n\text{NO}_3^- + n\text{NO}_2)} \quad (3)$$

$$\text{SOR} = \frac{n\text{SO}_4^{2-}}{(n\text{SO}_4^{2-} + n\text{SO}_2)} \quad (4)$$

Where NOR and SOR means nitrogen oxidation rate and sulfur oxidation rate, n refers to molar concentration. It can be easily deduced that larger NOR and SOR would generate more atmospheric aerosols, and atmospheric photolysis reaction of SO_2 would take place if the oxidation rate exceeds 0.1 (Ohta and Okita, 1990). In this study, NOR and SOR were always higher than 0.1 with averages of 0.14 and 0.27, respectively, suggesting that atmospheric oxidation of NO_2 and SO_2 contributed significantly to the formation of particulate matter. The mean NOR was comparable to that in Nanjing (0.16) during a long-lasting haze event but apparently lower than in Guangzhou (0.24), while the SOR was much higher than in Nanjing (0.13) but comparable to the value in Guangzhou (0.26) (Tan et al., 2009; Kang et al., 2013). Meanwhile, NO_2 surpassed SO_2 so strong with a mass ratio of 1.53, hence more atmospheric H_2O_2 and OH would be removed via reactions with NO_2 , and the formation of SO_4^{2-} would be greatly suppressed due to the competition effect (Puppe et al., 1993). Furthermore, the mass ratio of ambient nitrate to sulfate ($\text{NO}_3^-/\text{SO}_4^{2-}$) can help to track the relative importance of stationary versus mobile sources of nitrate and sulfur in the atmosphere (Yao et al., 2002). The stationary emission dominates in the sources of SO_2 and NO_2 if the ratio is less than 1.0, otherwise SO_2 and NO_2 mainly come from traffic activities (Huebert et al., 1988). Shanghai has been experiencing an increasing trend of $\text{NO}_3^-/\text{SO}_4^{2-}$ because of the very fast development of motor vehicles over

the past decade (Yao et al., 2002; Wang et al., 2006a; Fu et al., 2008). Therefore, more contribution of pollutants from mobile sources is expected to the local pollutions. The mean $\text{NO}_3^-/\text{SO}_4^{2-}$ during this **haze event** was 1.53, comparable to our early measurement in 2010 (1.61), but significantly higher than those observed in **haze events** in Guangzhou (1.02) and Nanjing (0.84 and 1.05) (Tan et al., 2009; Kang et al., 2013; Leng et al., 2013). The traffic-emitted SO_2 and NO_2 preponderating their stationary sources so conspicuous illustrated that the increasing traffic activities is one of main reasons for visibility degradation.

3.2 Formation and evolution of **haze event**

3.2.1 Atmospheric circle and synoptic situation

During winter time, the YRD region is often influenced by **cold** air from north, such as cold high pressure and cold front, and surface temperature inversion takes place sometimes (Chen et al., 2003; Liu et al., 2013). Under those conditions, atmospheric mixing and dispersion are basically weak in favor of pollutant accumulation, hence haze or fog easily occurs (Xu et al., 2011; Zhao et al., 2013).

The mean geopotential height **field** at 500 hPa revealed that during 1-10 December a long wave adjustment happened over the middle and high latitude of Eurasia. On 1 to 5, the atmospheric circulation in this region was representative of two troughs and one ridge, and these troughs were located in the west of the Balkhash lake and the north of Northeast China and a

wide ridge of high pressure existed between them (Figure 8). On 6, the circulation situation changed to two troughs and two ridges, and these troughs were located in the west of Lake Baikal and the east of Asia. However, over the central and southern China, there were flat westerly flows in most times with smaller radial degree and fast-moving short-wave troughs and ridges. During the **haze event**, the central and southern China was mainly under the stable westerly, and the YRD was affected by it. Additionally, at 700 hPa, the shear lines generated continuously and moved eastwards, and the difference between temperature and dew point mostly exceeded 4 °C, and the weak westerly and wind convergence appeared over the areas covered by haze clouds. At 850 hPa, the YRD was influenced by anticyclonic ring in most of time, wind speed smaller even static, and in view of temperature, this region was in one weak warm structure, isotherms relatively flat.

The surface weather maps at 6:00 (UTC) from 3-8 December are shown in Figure 9. A slowly migrating anti-cyclone (high-pressure) overlaid the YRD region and possibly caused a build-up of pollution due to the concomitant subsidence airflow and relatively stagnant conditions. The high pressure dominating this area also indicated aloft airflow convergence and surface divergence, which in turn would subside and restrict PBL development, and accordingly limit the **convection** of pollutants by trapping them within a shallow altitude. Unfavorable ambient temperature

posed another adverse effect on the thermal dynamic development of PBL height. The small pressure gradients over the YRD would horizontally suppress the air circulation at large scales because of low wind speed mostly below 2 m s^{-1} during the hazy episodes. Under those favorable situations, e.g. stable synoptic condition and calm wind, atmospheric pollutants were easily to accumulate within the surface atmospheric layer which ultimately led to severe urban air pollution. On the other hand, the YRD was sometime controlled by low pressure periphery and trough, and the pressure gradient was relatively weak. Although the low pressure was conducive to the rise of air masses, the vertical movement of upper and lower levels of the atmosphere was too weak to produce the effective dispersion of air pollutants and then result in pollution. Furthermore, the effect of ambient aerosols uptaking water vapor would effectively enhance their ability of scattering or absorbing solar radiation and damage atmospheric visibility eventually. The high ambient RH (60-80%) over this haze process indeed made a rich supply of water vapor for enhancing aerosol hygroscopic growth and was mostly responsible for the atmospheric visibility impairment. Normally, external forces such as high wind or rainfall are necessary to interrupt the stable situation and favor the diffusion of pollutants.

Over the target region ($30^{\circ} 40' \sim 31^{\circ} 53'$), during the **haze event**, the vertical winds almost were less than 0.4 Pa/s between 500 hPa and surface,

and it was less than 0.2 Pa/s at 700 hPa, implying that the vertical exchange of air parcels between the upper and lower atmospheric layers is very weak. Near the ground, the vertical velocity of winds was positive, and the relative vorticity was zero or negative value in most of time, demonstrating that airflow was prevailed in downdraft at the bottom of the atmosphere. Moreover, the temperature profile of sounding data revealed that the strong inversions occurred in 5 days with relatively low heights, so atmospheric convection and turbulence were inhibited, and then the blocked diffusion in vertical direction caused pollutant accumulation near the surface.

In summary, atmospheric pollutants were restricted within shallow layer, favorable for visibility impairment due to the dominance of weak high pressure system with low pressure gradients, subsidence airflow, unfavorable PBL height and meteorological situation. In good agreement with our study, Wu et al. (2005) reported that descending air motion and weak horizontal wind produced significantly high particle concentrations during a severe **haze event** in Guangzhou. Also in the YRD area, Fu et al. (2008) found that high pressure system responsible for stagnant conditions was the major reason of high pollution events. The stable synoptic condition and its long duration was indeed viewed as one of the most important factors ruling the formation and evolution of this **haze event**.

3.2.2 Impacts of air mass pathways

HYSPLIT-4 model, developed by the Air Resources Laboratory (ARL)

of the National Oceanic and Atmospheric Administration (NOAA) of USA (Draxler and Rolph, 2003), was employed to compute 48 h air mass backward trajectories at 500 m height, starting at 0:00 UTC and 12:00 UTC for each day. By doing so, we can identify and compile a full view of the possible source regions of pollutants.

According to those calculated trajectories plotted in Figure 10, three types of air mass pathways were determined in summary. Firstly, the air mass wandered inside the region with shallow atmospheric boundary layer, accounting for 60% of total trajectories, which was in good agreement with stable synoptic condition during the hazy episodes. This situation facilitates the accumulation of atmospheric pollutants and ultimately results in haze formation. Secondly, the subsidence flow from high altitude with minor horizontal movement, accounting for 30% of trajectories, dominated and brought in temporal clear sky between the hazy episodes on 2, 3 and 8 December. Thirdly, the air mass, originating from the northern inland China at high altitude, fast travelled southerly across the Northern China Plain (NCP) and the Eastern Region of China (ERC), and finally arrived in Shanghai over a long distance on 10 December, accounting for 10% of trajectories. They are helpful to dilute the atmospheric pollutants and then end this **haze event**. Most possibly, a combination of local emissions and long-distance transportation of remote emissions exerts the joint effects to the pollutants during the **haze event**.

3.2.3 Reduction of PBL height

PBL plays a vital role in determining the vertical dispersion of air pollutants that are emitted naturally or artificially from the Earth surface (Kim et al., 2007; Liu et al., 2013). Decreasing height of PBL can normally hold the pollutants within the shallow surface layer, suppress the vertical atmospheric dilution and ultimately **cause** regional environment shrouded by pollution (Kim et al., 2007). In Shanghai, several **field** measurements have monitored that PBL height is usually low during hazy episodes (Leng et al., 2014b; Zhang et al., 2015). By utilizing the normalized Lidar backscatter signal at 532 nm, the PBL retrieval at 30-sec resolution was derived in this study, and the time-height series was plotted in red line in **Figure 11**. Overall, PBL height was negatively correlated with atmospheric visibility with R^2 of 0.63, and averaged at 1.3 km during the clean periods and 0.6 km during the hazy episodes. From midday on 5 to the night on 6 December, the height of PBL decreased to 400 m lasting more than 30 hours, and $PM_{2.5}$ during this period enhanced to over $600 \mu\text{g m}^{-3}$, 5.4 times of the average of the **clean** periods. The lower PBL heights will retain more pollutants in the surface layer and cause the city surrounded by haze.

In theory, PBL basically evolves as a function of atmospheric thermal and dynamic factors, e.g. air temperature and wind speed (Liu et al., 2013). In fact, there is a feedback between atmospheric aerosol loading and PBL height. Briefly, the more ambient aerosols accumulate, the less solar

radiation reaches to surface, which inevitably poses a disadvantageous effect on surface air temperature as well as a positive impact on ambient RH, and further restricts the development of PBL. The low PBL height in turn forces the accumulation of aerosol particles in the high RH and shallow atmosphere, and ultimately degrade atmospheric visibility (Liu et al., 2013). Otherwise, more solar radiation arrives at the ground in case of clean sky, under those conditions the air temperature and PBL height increase while the ambient RH drops, which is unfavorable to the haze formation. This scientific issue involves many complicated atmospheric processes remaining poorly understood as well as deserving further study. As mentioned in Sect. 3.2.1 and 3.2.2, the YRD region was undergoing a large scale of weak high pressure with surface air moving slowly during the campaign. The air temperature retained at a low level which was not conducive to the development of PBL, thereby heavy air pollution took place and eventually resulted in visibility degradation. In short, the low PBL height is helpful for the **increase** of aerosol particles, hence favors the occurrence of **haze event**.

3.2.4 Aerosol composition and hygroscopicity

As important components of ambient particles, particle-phase water-soluble inorganic ions generally account for 30% of particulate matter in urban atmosphere, and are considered as a great contributor to the atmospheric visibility impairment because they hugely determine the

ability of aerosol particles to uptake water vapor (Hillamo et al., 1998; Andrews et al., 2000; Chow et al., 2006; Seinfeld and Pandis, 2006). Also, they are essential participants in the formation, growth and evolution of nanoparticles **by providing** significant potential of surface chemical reactions (Wang et al., 2006b). In Shanghai, sulfate and nitrate have been evidently identified as great contributors to the occurrence of heavy particulate pollution events (Wang et al., 2006b; Sun et al., 2006; Fu et al., 2008), and NH₃ **plays** a vital role in the enhancement of particulate sulfate and nitrate (Ye et al., 2011).

When ambient RH is high, those aerosols that are more hydrophilic can grow in diameter via uptaking water vapor, and through this way they can increase their ability of scattering light and cause atmospheric visibility impairment (Tang, 1996). A kappa value κ , describing particle hygroscopicity, was firstly introduced by Petters and Kreidenweis (2007) and employed here to investigate its relationship with haze formation. Assuming ambient aerosols are well internal-mixed, the effective integrated κ can be obtained through weighting their chemical compound volume fractions,

$$\kappa = \sum_i \varepsilon_i \kappa_i \quad (5)$$

where ε_i is the volume fraction of chemical compounds in particles, and κ_i is the effective κ of individual chemical composition. Equation (5) has been widely used and described elsewhere in detail (Petters and and

Kreidenweis., 2008; Yue et al., 2011; Leng et al., 2014a, 2014b). In this study, aerosol particle compositions were classified into three categories, and κ_i and ε_i for individual composition are listed in Table 1, of which “others” refers to $\text{PM}_{10}-(\text{SO}_4^{2-}+\text{NO}_3^-+\text{NH}_4^++\text{Cl}^-+\text{Na}^+)$, and is viewed as a chemical compound with $\kappa_i=0$ (Yue et al., 2011). **Figure 11** provides the time series of hourly-averaged kappa values, with higher κ during the hazy episodes (0.22) and lower κ during the clean periods (0.15), indicating that aerosols are basically more hygroscopic responsible for haze occurrence during the pollution period.

With the aim of better understanding the potential contribution of individual water-soluble ions, BC and ambient RH to atmospheric visibility impairment, we run nonlinear regression analysis and the results were plotted in **Figure 12**. The correlation between atmospheric visibility and individual ions, BC and $\text{PM}_{2.5}$ was not so impressive with R^2 from 0.11 to 0.22. However, it became more significant in view of ambient RH with R^2 of 0.41. The result suggests that the atmospheric visibility impairment is less driven by water-soluble ions but largely induced by hygroscopicity, in consistent with Tang (1996) and Roeland et al. (2014).

3.2.5 Aerosol size spectra

Atmospheric aerosol particles are usually divided into four classes according to their size distribution, i.e. nucleation mode (<25 nm), Aitken mode (25-100 nm), accumulation mode (100-1000 nm), and coarse mode

(>1000 nm) (Zhang et al., 2010). The ability to determine the amount of visible light scattered by atmospheric aerosols relies strongly on their number size distributions, of which accumulation mode plays the major role yet coarse and nucleation mode exert a minor contribution (Cheng et al., 2008b). Numerous studies have observed the inter-relationship between atmospheric visibility and aerosol number size distribution (Cheng et al., 2008; Roeland et al., 2014). To be more specific, Kang et al. (2013) reported that the expected reciprocal relationship was found only between atmospheric visibility and aerosols in 600-1400 nm instead of other sizes.

Accordingly, aerosol particles were classified into three categories, i.e. 10-600 nm, 600 nm-1.4 μm and 1.4-10 μm . By doing so, their nonlinear regression analysis with atmospheric visibility was computed and the results were given in Figure 13. As expected, no significant correlation was derived between atmospheric visibility and aerosol size of 10-600 nm and 1.4-10 μm , whereas aerosols in 600 nm-1.4 μm indeed controlled atmospheric visibility to a great extent with R^2 of 0.70, which further improved to 0.73 if we combined aerosol hygroscopic potential well determined by its size-resolved composition. In this study, aerosol number concentrations in 600 nm-1.4 μm were on average 110 cm^{-3} during the hazy episodes and 43 cm^{-3} during the clean periods. The atmospheric visibility was so dependent on aerosol number size distribution and its impairment

during the hazy episodes was mostly caused by the enhancement of aerosol concentration in 600 nm-1.4 μm .

4. Summary and conclusion

A historic **haze event** was fully analyzed for the temporal variations of aerosol optical, physical and chemical properties and meteorological conditions, as well as the formation and evolution mechanism. During the event, atmospheric visibility decreased dramatically, while particle burden, water-soluble inorganic ions, aerosol scattering and absorption coefficients increased evidently. In particular, particulate mass burden produced a new historic record by exceeding $600 \mu\text{g m}^{-3}$.

Many factors in combination drove the formation and evolution of this severe **haze event**. For most of the measured period, the YRD was under the control of a slowly migrating anti-cyclone to result in subsidence airflow and relatively stagnant conditions. The subsidence airflow suppressed vertical mixing and favored the accumulation of air pollutants within the shallow atmospheric layer. Moreover, the calm surface wind subsidence airflow was not constructive to the horizontal dispersion of air pollutants which further promoted the haze formation. In summary, the significant increase of regional pollutants from anthropogenic emissions was the basic cause of this haze formation, and the unfavorable meteorological conditions played as the external reason.

Acknowledgements

This research is supported by the National Key Technology R&D Program of Ministry of Science and Technology (2014BAC16B01), the National Natural Science Foundation of China (41475109), and partly by the Jiangsu Collaborative Innovation Center for Climate Change, and the Key Laboratory for Aerosol-Cloud-Precipitation of China Meteorological Administration (KDW1401) and the Laboratory of Meteorological Disaster of Ministry of Education (KLME1416).

Reference

- Andrews, E., Saxena, P., Mussara, S., Hildemann, L. M., Koutrakis, P., McMurry, P. H., Olmez, I., and White, W. H.: Concentration and composition of atmospheric aerosols from the 1995 SEAVS experiment and a review of the closure between chemical and gravimetric measurements, *Journal of the Air&Waste Management Association*, 50, 648-664, 2000.
- Bell, M. L., Cifuentes, L. A., Davis, D. L., Cushing, E., and Telles, A. G.: Gouveia, N. Environmental health indicators and a case study of air pollution in Latin American cities, *Environ. Res.*, 111, 57-66, 2011.
- Bergin, M., Cass, G. R., Xu, J., Fang, F., Zeng, L. M., Yu T., Salmon, L. G., Kiang, C. S., Tang, X. Y., Zhang, Y. H., and Chameides, W. L.:

-
- Aerosol radiative, physical, and chemical properties in Beijing during June 1999, *J. Geophys. Res.*, 106, 17969–17980, 2001.
- Boers, R., and Eloranta, E.W.: Lidar measurements of the atmospheric entrainment zone and the potential temperature jump across the top of the mixed layer, *Bound.-Lay. Meteorol.*, 34, 357–375, 1986.
- Bond, T. C. and Bergstrom R. W.: Light Absorption by Carbonaceous Particles: An Investigative Review, *Aerosol Sci. Technol.*, 40, 27–47, 2006.
- Brooks, I. M.: Finding boundary layer top: application of a wavelet covariance transform to lidar backscatter profiles, *J. Atmos. Ocean. Tech.*, 20, 1092–1105, 2003.
- Campbell, J. R., Hlavka, D. L., Welton, E. J., Flynn, C. J., Turner, D. D., Spinhirne, J. D., Scott, V. S., and Hwang, I. H.: Full-time, eye-safe cloud and aerosol lidar observation at atmospheric radiation measurement program sites: Instruments and data processing, *J. Atmos. Ocean Technol.*, 19, 431–442, 2002.
- Cao J, Xu H, Xu Q, et al. Fine particulate matter constituents and cardiopulmonary mortality in a heavily polluted Chinese city, *J. Environmental health perspectives*, 120, 373-378, 2012.
- Che, H. Z., Zhang, X. Y., Li, Y., Zhou, Z. J., Qu, J. J., Hao, X. J.: Haze trends over the capital cities of 31 provinces in China, 1981–2005, *Theor. Appl. Climatol.*, 97, 235–242, 2009.

Chen, L. W. A., Chow, J. C., Doddridge, B. G., Dickerson, R. R., Ryan, W. F., and Mueller, P. K.: Analysis of a summertime PM_{2.5} and haze episode in the mid-Atlantic region, *J. Air Waste Manage. Assoc.*, 53, 946–956, 2003.

Cheng, T. T., Han, Z. W., Zhang, R. J., Du, H. H., Jia, X., Wang, J. J., and Yao, J. Y.: Black carbon in a continental semi-arid area of Northeast China and its possible sources of fire emission, *J. Geophys. Res.*, 115, D23204, doi:10.1029/2009JD013523, 2010.

Cheng, Y. F., Wiedensohler, A., Eichler, H., Heintzenberg, J., Tesche, M., Ansmann, A., Wendisch, M., Su, H., Althausen, D., Herrmann, H., Gnauk, T., Brüggemann, E., Hu, M., and Zhang, Y. H.: Relative humidity dependence of aerosol optical properties and direct radiative forcing in the surface boundary layer at Xinken in Pearl River Delta of China: An observation based numerical study, *Atmos. Environ.*, 42, 6373–6397, 2008a.

Cheng, Y. F., Wiedensohler, A., Eichler, H., Su, H., Gnauk, T., Brüggemann, E., Herrmann, H., Heintzenberg, J., Slanina, J., Tuch, T., Hu, M., and Zhang, Y. H.: Aerosol optical properties and related chemical apportionment at Xinken in Pearl River Delta of China, *Atmos. Environ.*, 42, 6351–6372, 2008b

Chow, J. C., Chen, L. W. A., Watson, J. G., Lowenthal, D. H., Magliano, K. A., Turkiewicz, K., and Lehrman, D. E.: PM_{2.5} chemical composition

-
- and spatiotemporal variability during the California regional PM10/PM2.5 air quality study (CRPAQS), *J. Geophys. Res.*, 111, D10S04, 2006.
- Cohn, S. A., Angevine, W. M.: Boundary layer height and entrainment zone thickness measured by lidars and wind-profiling radars, *J. Appl. Meteorol.*, 39, 1233–1247, 2000.
- Draxler, R. R. and Rolph, G. D.: HYSPLIT (Hybrid Single-Particle Lagrangian Integrated Trajectory) Model access via NOAA ARL READY Website (<http://www.arl.noaa.gov/ready/hysplit4.htm>), NOAA Air Resources Laboratory, Silver Spring, MD, 2003.
- Du, H. H., Kong, L. D., Cheng, T. T., Chen, J. M., Du, J. F., Li, L., Xia, X. G., Leng, C. P., and Huang, G. H.: Insights into summertime haze pollution events over Shanghai based on online water-soluble ionic composition of aerosols, *Atmos. Environ.*, 45, 51311-5137, 2011.
- ~~Dumka, U. C., Krishna Moorthy, K., Kumar, R., Hegde, P., Sagar, R., Pant, P., Singh, N., and Suresh Babu, S.: Characteristics of aerosol black carbon mass concentration over a high altitude location in the Central Himalayas from multi-year measurements, *Atmos. Res.*, 96, 510–521, 2010.~~
- Fu, Q. Y., Zhuang, G. S., Wang, J., Xu, C., Huang, K., Li, J., Hou, B., Lu, T., and Streets, D. G.: Mechanism of formation of the heaviest pollution episode ever recorded in the Yangtze River Delta, China, *Atmos. Environ.*, 42, 2023–2036, 2008.

Gao, J., Wang, T., Zhou, X. H., Wu, W. S., and Wang, W. X.: Measurement of aerosol number size distributions in the Yangtze River delta in China: formation and growth of particles under polluted conditions, *Atmos. Environ.*, 43, 829–836, 2009.

Hansen, A. D. A., Rosen, H., and Novakov, T.: The aethalometer-an instrument for the real-time measurement of optical absorption by aerosol particles, *Sci. Total Environ.*, 36, 191–196, 1984.

~~He, Q. S., Li, C. C., Mao, J. T., Lau, A. K. H., and Li, P. R.: A study on the aerosol extinction to backscatter ratio with combination of micro-pulse LIDAR and MODIS over Hong Kong, *Atmos. Chem. Phys.*, 6, 3243–3256, doi:10.5194/acp-6-3243-2006, 2006.~~

Hillamo, R., Allegrini, I., Sparapani, R., and Kerminen, V.M.: Mass size distributions and precursor gas concentrations of major inorganic ions in Antarctica aerosol, *International Journal of Environmental Analytical Chemistry*, 71, 357-369, 1998.

Huebert, B. J., Bates, T., Russell, P. B., Shi, G. Y., Kim, Y. J., Kawamura, K., Carmichael, G., and Nakajima, T.: An overview of ACE-Asia: Strategies for quantifying the relationships between Asian aerosols and their climatic impacts, *J. Geophys. Res.*, 108, 1–20, 2003.

Huebert, B. J., Wang, M. X., Lv, W. X.: Atmospheric nitrate, sulfate, ammonium and calcium concentrations in China, *Tellus B* <http://dx.doi.org/10.1111/j.1600-0889.1988.tb00296.x>, 1988.

IPCC: Climate Change 2013: The Physical Science Basis. Contribution of Working Group I to the Fifth Assessment Report of the Intergovernmental Panel on Climate Change, edited by: Jousaume, S. Penner, J., and Tangang, F., IPCC, Stockholm, 2013.

Kang, H. Q., Zhu, B., Su, J. F., Wang, H. L., Zhang, Q. C., and Wang, F.: Analysis of a long-lasting haze episode in Nanjing, China, *Atmos. Res.*, 120-121, 78-87, 2013.

Kim, S. W., Yoon, S. C., Won, J. G., and Choi, S. C.: Ground-based remote sensing measurements of aerosol and ozone in an urban area: A case study of mixing height evolution and its effect on ground-level ozone concentrations, *Atmos. Environ.*, 41, 7069-7081, 2007.

Lance, S., Medina, J., Smith, J. N., and Nenes, A.: Mapping the operation of the DMT Continuous Flow CCN counter, *Aerosol Sci. Tech.*, 40, 242–254, 2006

Leng, C. P., Cheng, T. T., Chen, J. M., Zhang, R. J., Tao, J., Huang, G. H., Zha, S. P., Zhang, M. G., Fang, W., Li, X., and Li, L.: Measurements of surface cloud condensation nuclei and aerosol activity in downtown Shanghai, *Atmos. Environ.*, 69, 354–361, 2013.

Leng, C. P., Zhang, Q., Zhang, D. Q., Xu, C., Cheng, T. T., Zhang, R. J., Tao, J., Chen, J. M., Zha, S. P., Zhang, Y. W., Li, X., and Kong, L. D.: Variations of Cloud Condensation Nuclei (CCN) and Aerosol Activity during Fog-Haze Episode: a Case Study from Shanghai, *Atmos. Chem. &*

-
- Phys., 14, 12499-12512, 2014a.
- Leng, C. P., Zhang, Q., Tao, J., Zhang, H. F., Zhang, D. Q., Xu, C., Li, X., Kong, L. D., Cheng, T. T., Zhang, R. J., Yang, X., Chen, J. M., Qiao, L. P., Lou, S. R., Wang, H. L., and Chen, C. H.: Impacts of New Particle Formation on Aerosol Cloud Condensation Nuclei (CCN) Activity in Shanghai: Case Study, *Atmos. Chem. & Phys.*, 14, 11353-11365, 2014b.
- Lee, D. O.: Trends in summer visibility in London and Southern England 1962–1979, *Atmos. Environ.*, 17, 151–159, 1983.
- Li, C., Lau, K. H., Mao, J., and Chu, D. A.: Retrieval, validation and application of the 1-km aerosol optical depth from MODIS measurements over Hong Kong, *IEEE T. Geosci. Remote*, 43, 2650–2658, 2005.
- Liu, X. G., Li, J., Qu, Y., Han, T., Hou, L., Gu, J., Chen, C., Yang, Y., Liu, X., Yang, T., Zhang, Y., Tian, H., and Hu, M.: Formation and evolution mechanism of regional haze: a case study in the megacity Beijing, China, *Atmos. Chem. Phys.*, 13, 4501-4514, 2013.
- Lohmann, U. and Feichter, J.: Global indirect aerosol effects: a review, *Atmos. Chem. Phys.*, 5, 715–737, doi:10.5194/acp-5-715-2005, 2005.
- Malm, W. C. and Day, D. E.: Estimates of aerosol species scattering characteristics as a function of relative humidity, *Atmos. Environ.*, 35, 2845-02860, 2001.
- McNulty, R. P.: The effect of air pollutants on visibility in fog and haze at New York city, *Atmos. Environ.*, 2, 625–628, 1968.

-
- Menut, L., Flamant, C., Pelon, J., and Flamant, P. H.: Urban boundary-layer height determination from lidar measurements over the Paris area, *Appl. Optics*, 38, 945–954, 1999.
- Ohta, S., Okita, T.: A chemical characterization of atmospheric aerosol in Sapporo, *Atmos. Environ.*, 24A, 815-822, 1990.
- Petters, M. D. and Kreidenweis, S. M.: A single parameter representation of hygroscopic growth and cloud condensation nucleus activity, *Atmos. Chem. Phys.*, 7, 1961–1971, doi:10.5194/acp-7-1961-2007, 2007.
- Petzold, A., Kopp, C., and Niessner, R.: The dependence of the specific attenuation cross-section on black carbon mass fraction and particle size, *Atmos. Environ.*, 31, 661–672, 1997.
- Poppe, D., Wallasch, M., Zimmermann, J.: The dependence of the concentration of OH on its precursors under moderately polluted conditions: a model study, *J. Atmos. Chem.*, 16, 61-78, 1993.
- Ritesh, G., Christina, H., Menas. Kafatos., Si-Chee. T.: Influences of winter haze on fog/low cloud over the Indo-Gangetic plains, *J. Geophys. Res.*, 112, D05207, doi:10.1029/2005JD007036, 2007.
- Roberts, G. C. and Nenes, A.: A continuous-flow streamwise thermal-gradient CCN chamber for atmospheric measurements, *Aerosol Sci. Tech.*, 39, 206–221, 2006.
- Schichtel, B. A., Husar, R. B., Falke, S. R., and Wilson, W. E.: Haze trends over the United States, 1980–1995, *Atmos. Environ.*, 35, 5205–5210,

2001.

Sun, Y. L., Zhuang, G. S., Wang, Y., Han, L. H., Guo, J. H., Dan, M., Zhang, W. J., Wang, Z. F., and Hao, Z. P.: The air-borne particulate pollution in Beijing-Concentration, composition, distribution and sources, *Atmos. Environ.*, 38, 5991–6004, 2004.

Sun, Y. L., Zhuang, G. S., Tang, A. H., Wang, Y., and An, Z. S.: Chemical characteristics of PM_{2.5} and PM₁₀ in haze-fog Episodes in Beijing, *Environ. Sci. Technol.*, 40, 3148–3155, 2006

Quinn, P. K. and Bates, T.: North American, Asian, and Indian haze: Similar regional impacts on climate?, *Geophys. Res. Lett.*, 30, 1555, doi:10.1029/2003GL016934, 2003.

Seinfeld, J. H., and Pandis, S. N.: *Atmospheric Chemistry and Physics: From Air Pollution to Climate Change*, second ed. John Wiley & Sons, New York, USA, 57-58 and 381-383, 2006.

Tan, H. H., Duan, J. C., He, K. B., Ma, Y. L., Duan, F. K., Chen, Y., Fu, J. M.: Chemical characteristics of PM_{2.5} during a typical haze episode in Guangzhou, *J. Environ. Sci.*, 21, 774-781, 2009.

Tang, I. N.: Chemical and size effects of hygroscopic aerosols on light scattering coefficients, *J. Geophys. Res.*, 101, 19245–19250, 1996.

Tie, X. X., Wu, D., and Brasseur, G.: Lung cancer mortality and exposure to atmospheric aerosol particles in Guangzhou, China, *Atmos. Environ.*, 43, 2375–2377, 2009.

-
- Wang, Y., Zhuang, G. S., Zhang, X. Y., Huang, K., Xu, C., Tang, A. H., Chen, J. M., An, Z. S.: The ion chemistry, seasonal cycle, and sources of PM_{2.5} and TSP aerosol in Shanghai, *Atmos. Environ.*, 40, 2935-2952, 2006a.
- Wang, Y., Zhuang, G. S., Sun, Y. L., and An, Z. S.: The variation of characteristics and formation mechanisms of aerosols in dust, haze, and clear days in Beijing, *Atmos. Environ.*, 40, 6579–6591, 2006b.
- Weingartner, E., Saathoff, H., Schnaiter, M., Streit, N., Bitnar, B., and Baltensperger, U.: Absorption of light by soot particles: determination of the absorption coefficient by means of aethalometers, *J. Aerosol Sci.*, 34, 1445-1463, 2003.
- Welton E.J., Voss K.J., Quinn P. K., Flatau P. J., Markowicz K., Campbell J. R., Spinhirne J.D., Gordon H.R., Johnson, J. E., Measurements of aerosol vertical profiles and optical properties during INDOEX 1999 using micropulse lidars, *J. Journal of Geophysical Research: Atmospheres*, 107, doi: 10.1029/2000JD000038, 2002.
- Welton E.J., Campbell J.R., Micropulse lidar signals: Uncertainty analysis, *J. Journal of Atmospheric and Oceanic Technology*, 19, 2089-2094, 2002.
- Woo, K. S., Chen, D. R., Pui, D. Y. H., McMurry, P. H.: Measurements of Atlanta aerosol size distributions: observations of ultrafine particle events, *Aerosol Sci. Technol.*, 34, 75-87, 2001.
- Wu, D., Bi, X., Deng, X., Li, F., Tan, H., Liao, G., and Huang, J.: Effects

-
- of atmospheric haze on the deterioration of visibility over the Pearl River Delta, *Acta Meteorol. Sin.*, 64, 510–517, 2006.
- Wu, D., Tie, X., Li, C., Ying, Z., Lau, A. K.-H., Huang, J., Deng, X., and Bi, X.: An extremely low visibility event over the Guangzhou region: a case study, *Atmos. Environ.*, 39, 6568–6577, 2005.
- Xiao, F., Brajer, V., and Mead, R. W.: Blowing in the wind: the impact of China's Pearl River Delta on Hong Kong's air quality, *Sci. Total Environ.*, 367, 96–111, 2006.
- Xu, W. Y., Zhao, C. S., Ran, L., Deng, Z. Z., Liu, P. F., Ma, N., Lin, W. L., Xu, X. B., Yan, P., He, X., Yu, J., Liang, W. D., and Chen, L. L.: Characteristics of pollutants and their correlation to meteorological conditions at a suburban site in the North China Plain, *Atmos. Chem. Phys.*, 11, 4353–4369, doi:10.5194/acp-11-4353-2011, 2011.
- Yao, X. H., Chan, C. K., Fang, M., Cadle, S., Chan, T., Mulawa, P., He, K. B., Ye, B. M.: The water-soluble ionic composition of PM_{2.5} in Shanghai and Beijing, China, *Atmos. Environ.*, 36, 4223–4234, 2002.
- Ye, X. N., Ma, Z., Zhang, J. C., Du, H. H., Chen, J. M., Chen, H., Yang, X., Gao, W., and Geng, F. H.: Important role of ammonia on haze formation in Shanghai, *Environ. Res. Lett.*, 6, doi: 10.1088/1748-9326/6/2024019, 2011.
- Yue, D. L., Hu, M., Zhang, R. J., Wu, Z. J., Su, H., Wang, Z. B., Peng, J. F., He, L. Y., Huang, X. F., Gong, Y. G., and Wiedensohler, A.: Potential

contribution of new particle formation to cloud condensation nuclei in Beijing, *Atmos. Environ.*, 45, 6070–6077, 2011.

Zhang, M., Wang, X. M., Chen, J. M., Cheng, T. T., Wang, T., Yang, X., Gong, Y. G., Geng, F. H., and Chen, C. H.: Physical characterization of aerosol particles during the Chinese New Year's firework events, *Atmos. Environ.*, 44, 5191–5198, 2010.

Zhang, Q. C., Zhu, B., Su, J. F., Wang, H. L.: Characteristics of aerosol water-soluble inorganic ions in three types air-pollution incidents of Nanjing City, *Environ. Sci.*, 33(6), 1944-1951, 2012 (in Chinese).

Zhao, P. S., Dong, F., He, D., Zhao, X. J., Zhang, X. L., Zhang, W. Z., Yao, Q., and Liu, H. Y.: Characteristics of concentrations and chemical compositions for PM_{2.5} in the region of Beijing, Tianjin, and Hebei, China, *Atmos. Chem. Phys.*, 13, 4631–4644, doi:10.5194/acp-13-4631-2013, 2013

Zhao, X. J., Zhao, P. S., Xu, J., Meng, W., Pu, W. W., Dong, F., He, D., and Shi, Q. F.: Analysis of a winter regional haze event and its formation mechanism in the North China Plain, *Atmos. Chem. Phys.*, 13, 5685-5696, 2013.

Table 1. Effective hygroscopicity parameters (κ) and densities of the three category compositions.

Species	Data source	κ	Density (g cm^{-3})
Sulfate & nitrate	$\text{SO}_4^{2-} + \text{NO}_3^- + \text{NH}_4^+$	0.6	1.7
Sodium chloride	$\text{Cl}^- + \text{Na}^+$	1	2.2
Insoluble compounds	Others	0	2.0

Figure captions:

Figure 1. (a) Temporal variations of $PM_{2.5}$, PM_{10} and atmospheric visibility (vis) measured in Shanghai from 1 to 10 December 2013. The dash line is vis at 10 km. (b) and (c) show temporal variations of meteorological parameters from 1 to 10 December 2013.

Figure 2. Temporal variations of $PM_{2.5}$ in Hangzhou, Nanjing and Hefei (a) and their mean concentrations from 1 to 10 December 2013.

Figure 3. Aerosol optical depth (AOD) at 550 nm from MODIS over the YRD region at 6:00 (UTC) from 1 to 10 December 2013 (<http://modis.gsfc.nasa.gov/>).

Figure 4. Temporal variations of black carbon (BC) concentration, aerosol scattering (Sc) and absorptive (Ab) coefficients from 1 to 10 December 2013.

Figure 5. (a) Time series of 4-min mean aerosol number size spectra and aerosol number concentration (pink line) and (b) averaged aerosol number size distribution from 5 to 10 December 2013.

Figure 6. Time series of 1 h mean CCN concentration (N_{CCN}) at supersaturations (SS) of 0.2-1.0% from 6 to 10 December 2013.

Figure 7. Temporal variations of chemical species in particles from 1 to 10 December 2013.

Figure 8. Atmospheric circulation situation at 500 hPa and 850 hPa from 3 to 6 December 2013.

Figure 9. Surface weather maps from 3 to 8 December 2013. The black star denotes the measurement site (<http://qixiangxinxifabupingtai.ejinqiao.com>).

Figure 10. Air mass 48-h backward trajectories arriving at Shanghai from 1 to 10 December 2013. A new trajectory is started at 0:00 (UTC) and calculated every 24 h.

Figure 11. Time series of 1-h mean kappa value (i.e. κ) and 5-min mean PBL height from 1 to 10 December.

Figure 12. Scatter plots of RH, BC, $PM_{2.5}$ and inorganic ions in particles versus atmospheric visibility.

Figure 13 Scatter plots of aerosol number concentrations in ranges of 0.01-0.6 μm , 0.6-1.4 μm and 1.4-10 μm , and aerosol number concentration multiplied by particle hygroscopicity (kappa value, κ) versus atmospheric visibility.

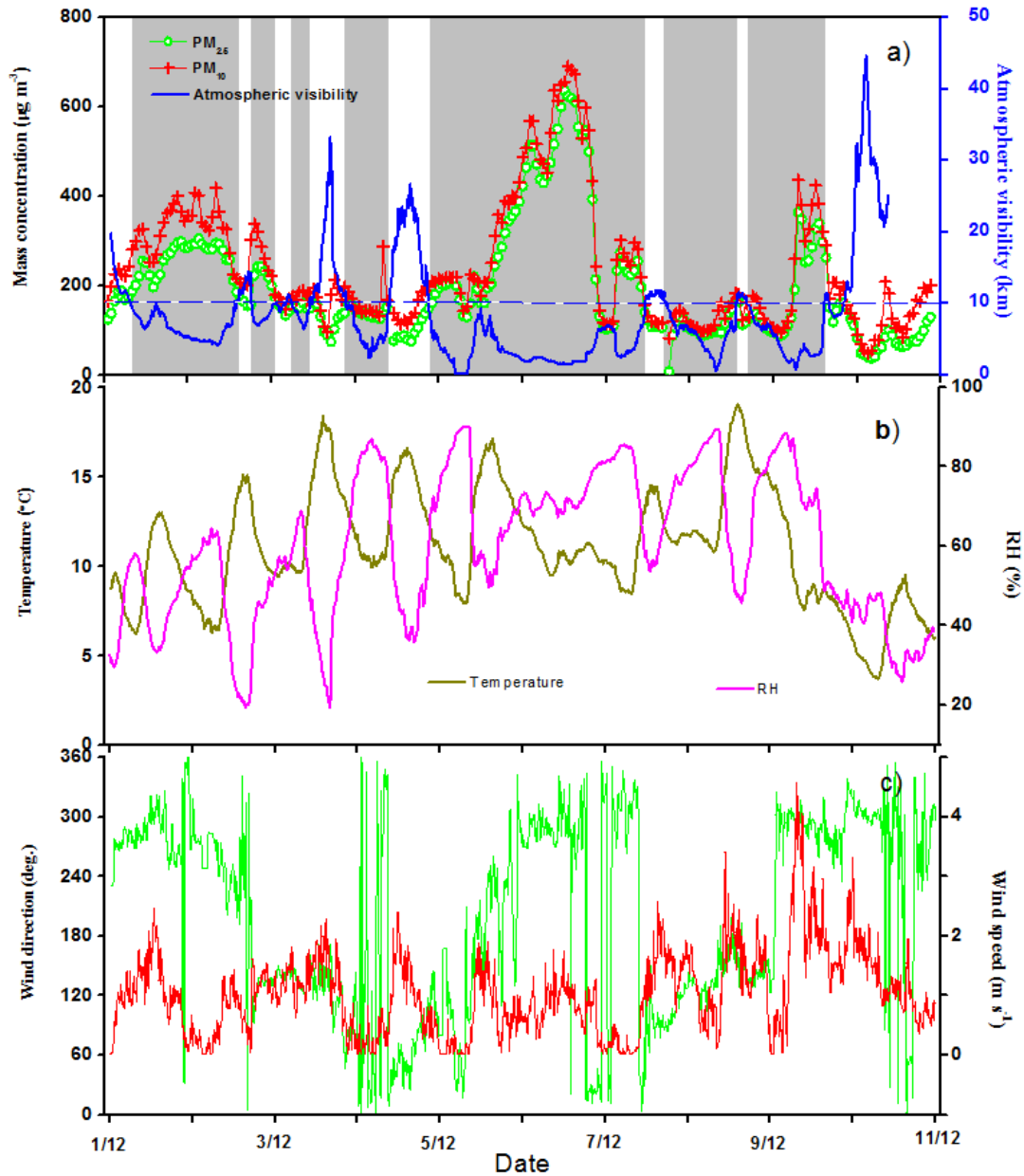


Figure 1(a) Temporal variations of $PM_{2.5}$, PM_{10} and atmospheric visibility (vis) measured in Shanghai from 1 to 10 December 2013. The dash line is vis. at 10 km. (b) and (c) show temporal variations of meteorological parameters from 1 to 10 December 2013.

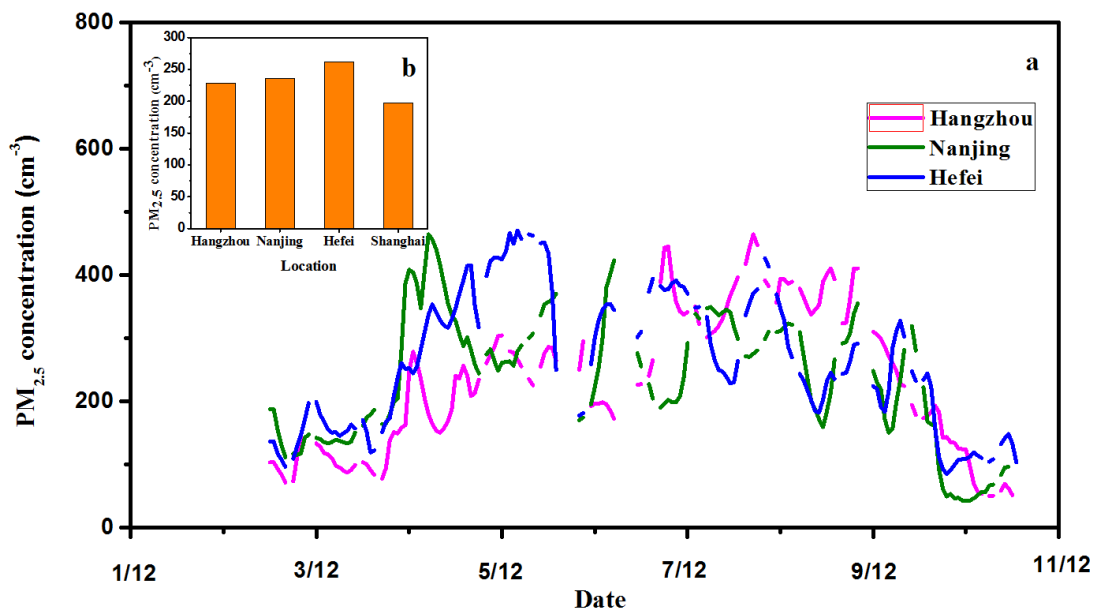


Figure 2 Temporal variations of PM_{2.5} in Hangzhou, Nanjing and Hefei (a) and their mean concentrations (b) from 1 to 10 December 2013.

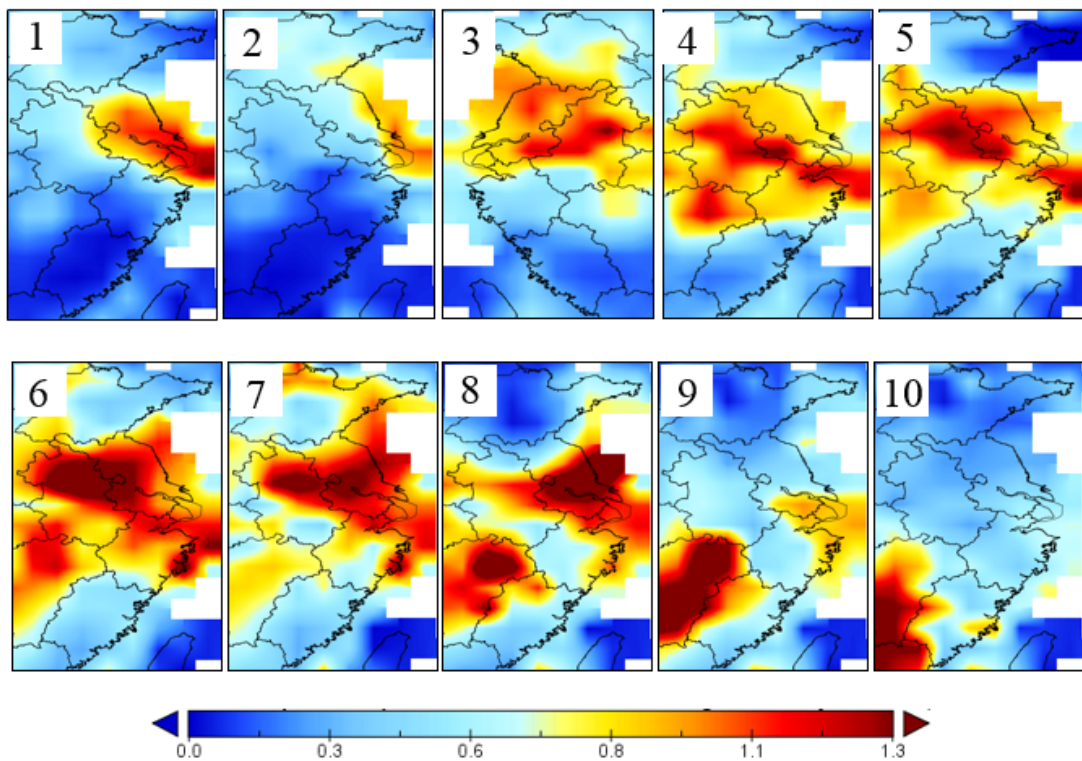


Figure 3 Aerosol optical depth (AOD) at 550 nm from MODIS over the YRD region at 6:00 (UTC) from 1 to 10 December 2013 (<http://modis.gsfc.nasa.gov/>).

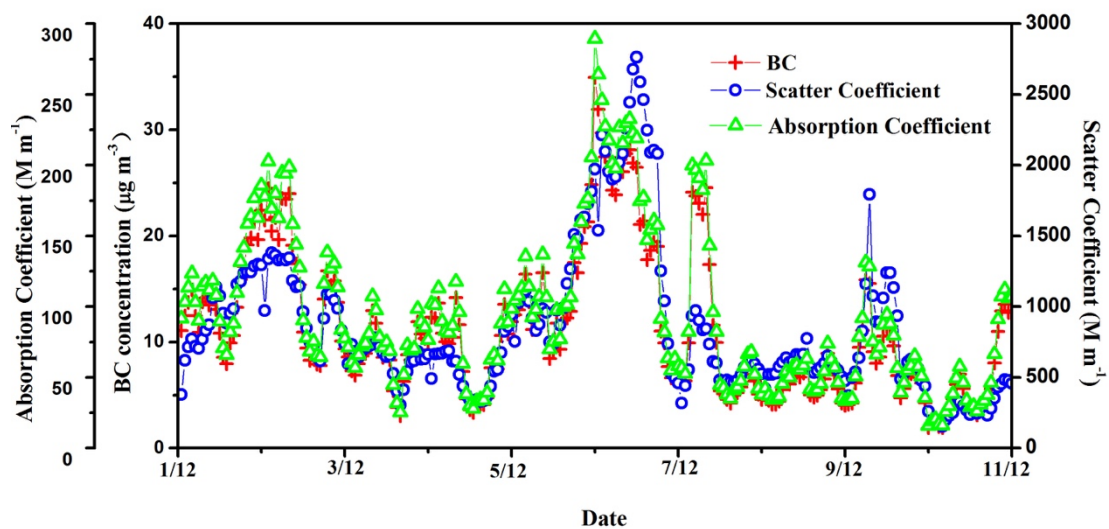


Figure 4 Temporal variations of black carbon (BC) concentration, aerosol scattering (Sc) and absorptive (Ab) coefficients from 1 to 10 December 2013.

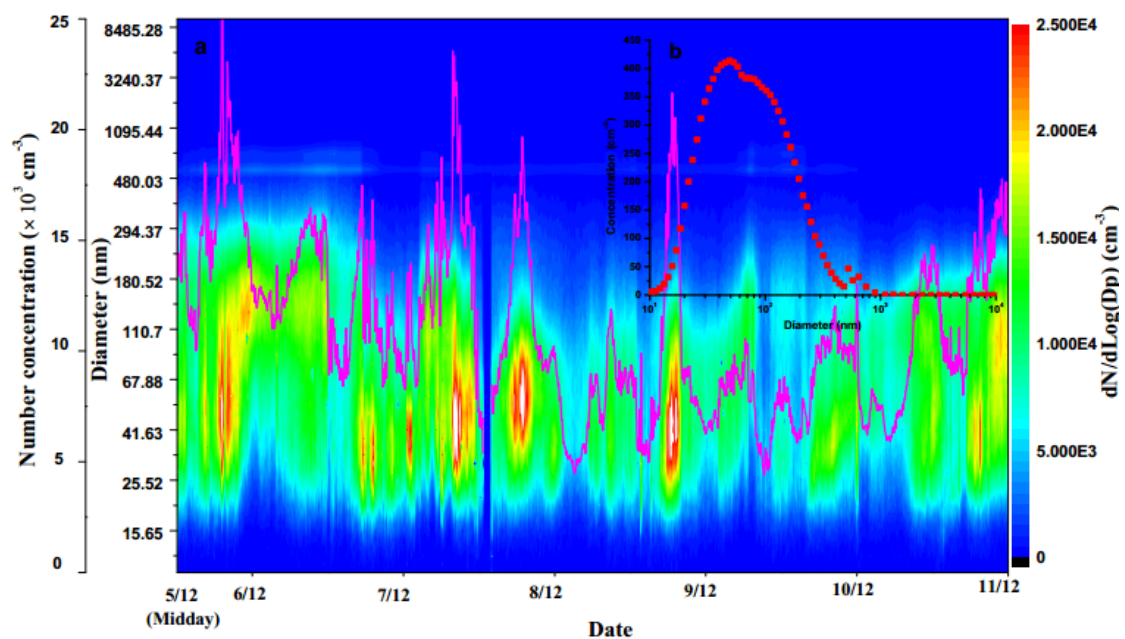


Figure 5 Time series of 4-min mean aerosol number size spectra and integrating number concentration (pink line, a) and averaged aerosol number size distribution (b) from 5 to 10 December 2013.

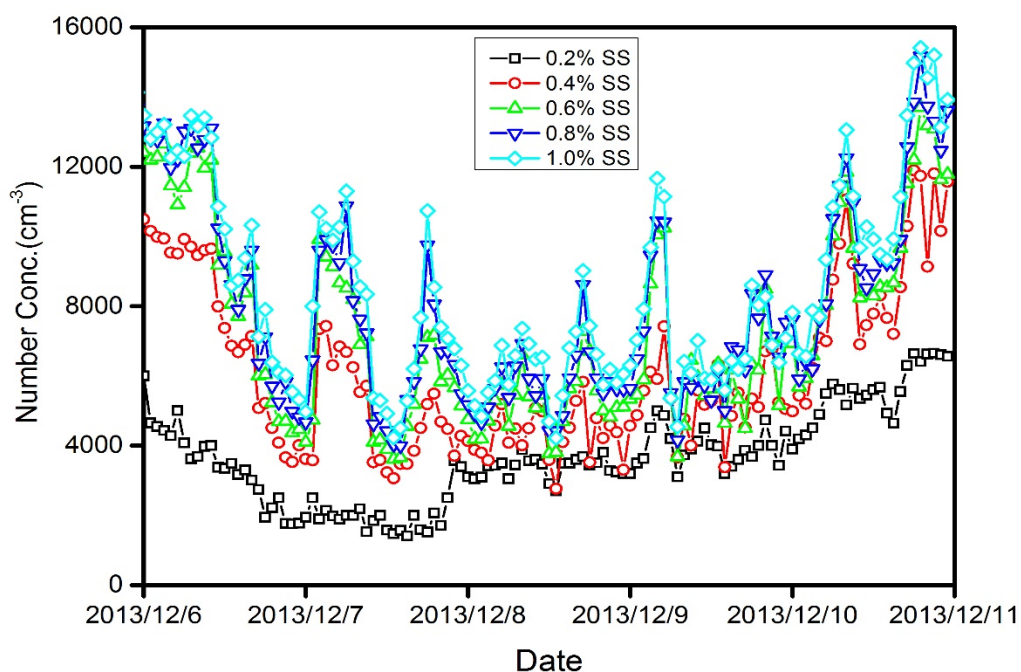


Figure 6 Time series of 1 h mean CCN concentration (N_{CCN}) at supersaturations (SS) of 0.2-1.0% from 6 to 10 December.

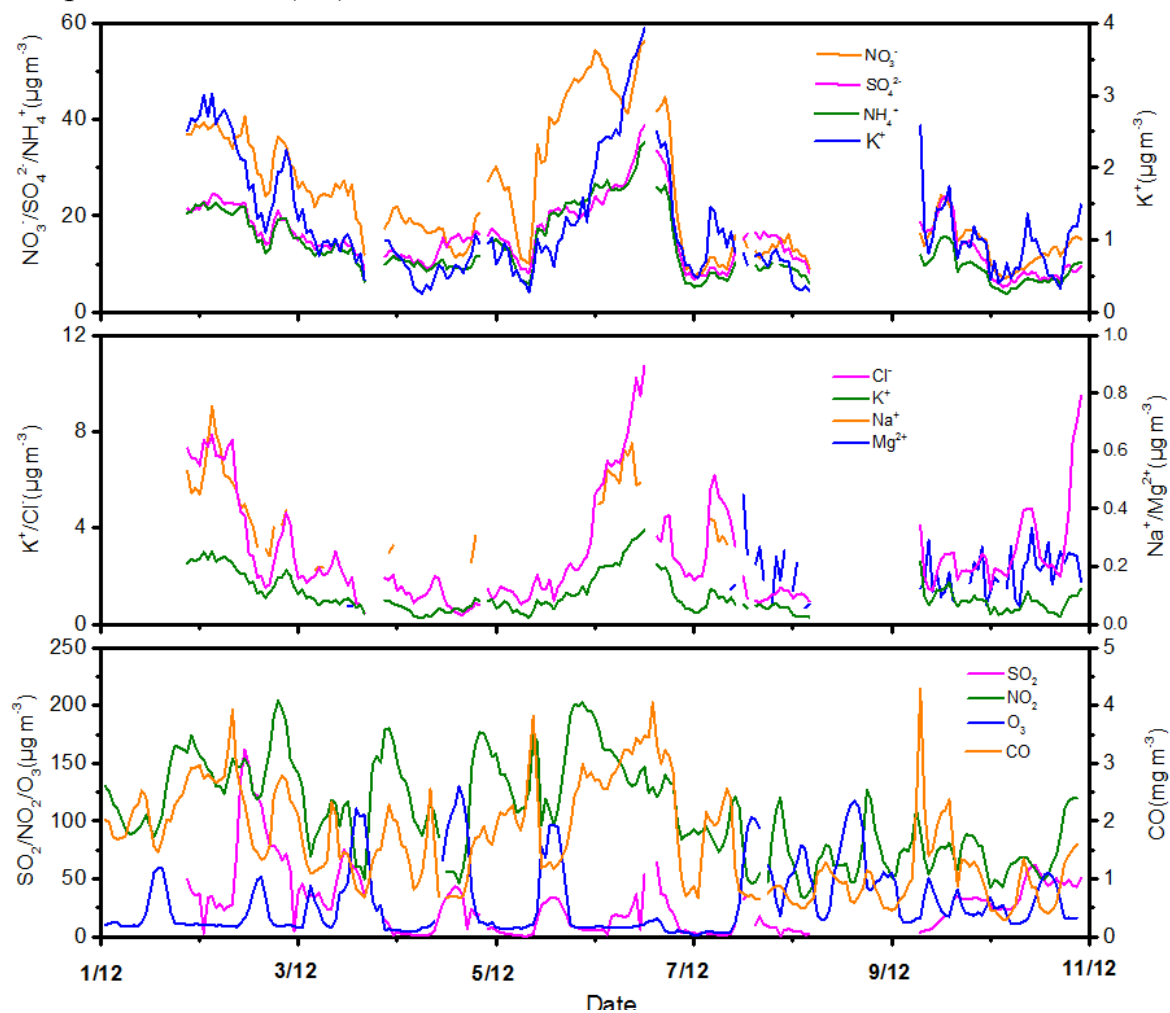


Figure 7 Temporal variations of chemical species in particles from 1 to 10 December 2013.

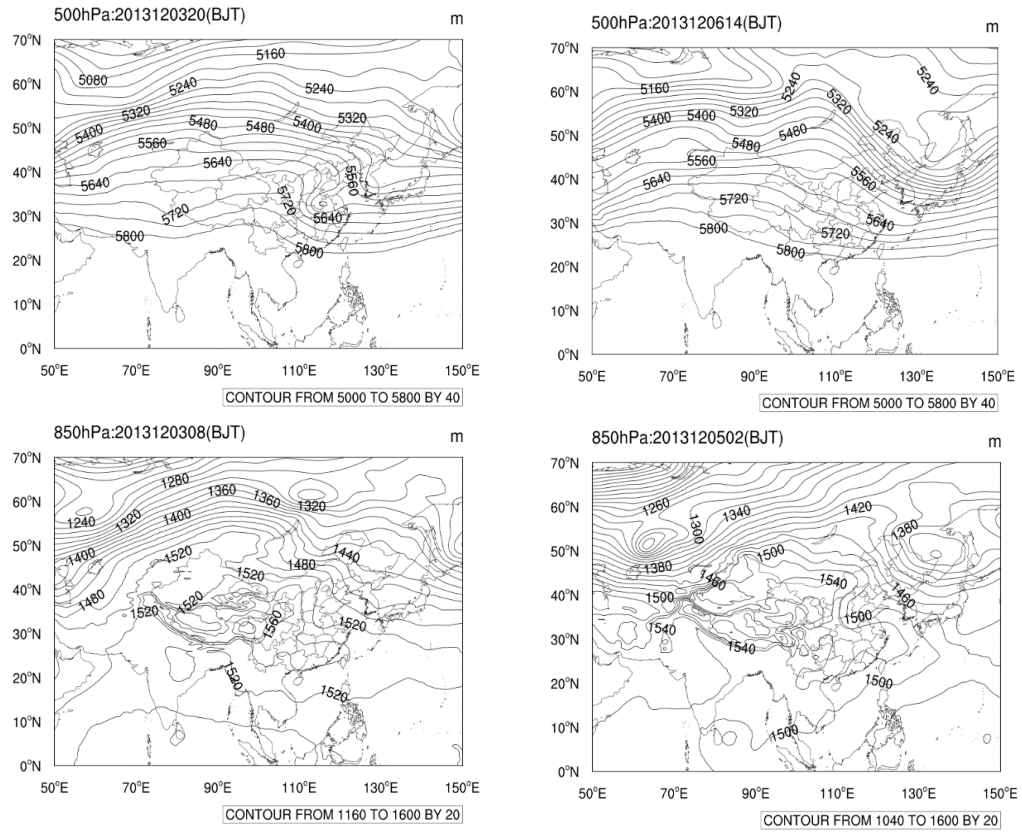


Figure 8 Atmospheric circulation situation at 500 hPa and 850 hPa from 3 to 6 December 2013.

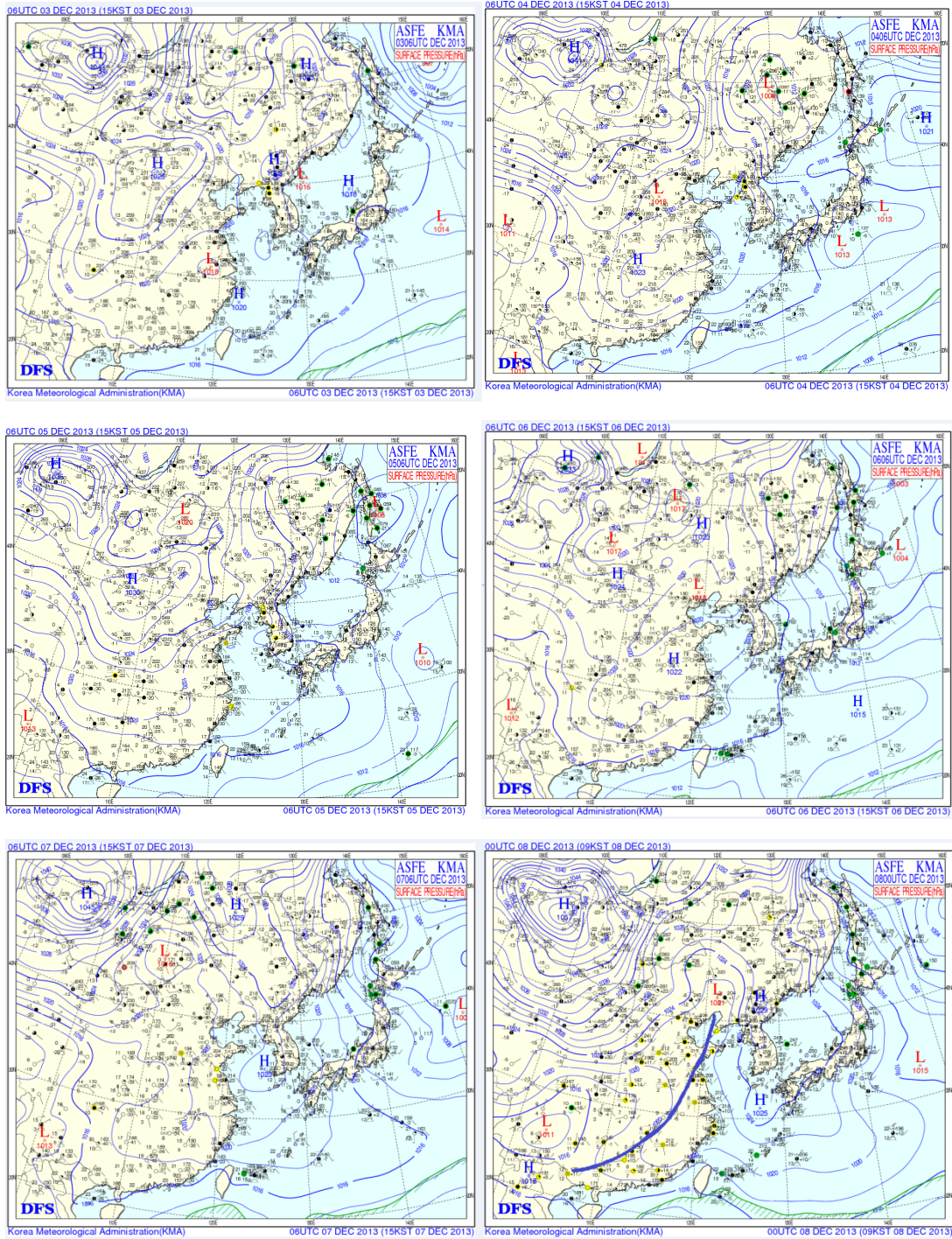


Figure 9 Surface weather maps at 6:00 (UTC) from 3 to 8 December 2013.

The black star denotes the measurement site (<http://qixiangxinxfabupingtai.ejinqiao.com>).

NOAA HYSPLIT MODEL
Backward trajectories ending at 0000 UTC 10 Dec 13
GDAS Meteorological Data

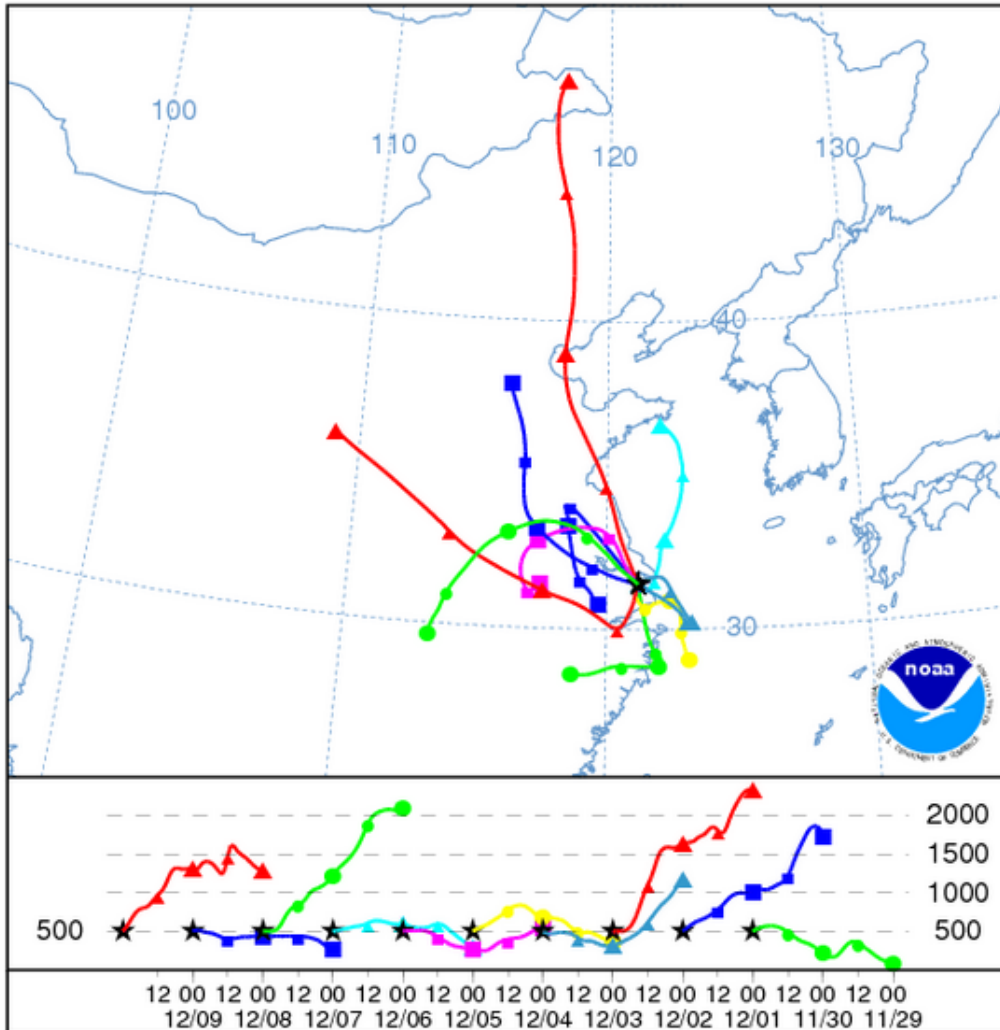


Figure 10 Air mass 48-h backward trajectories arriving at Shanghai from 1 to 10 December 2013 (500 m). A new trajectory is started at 0:00 (UTC) and calculated every 24 h.

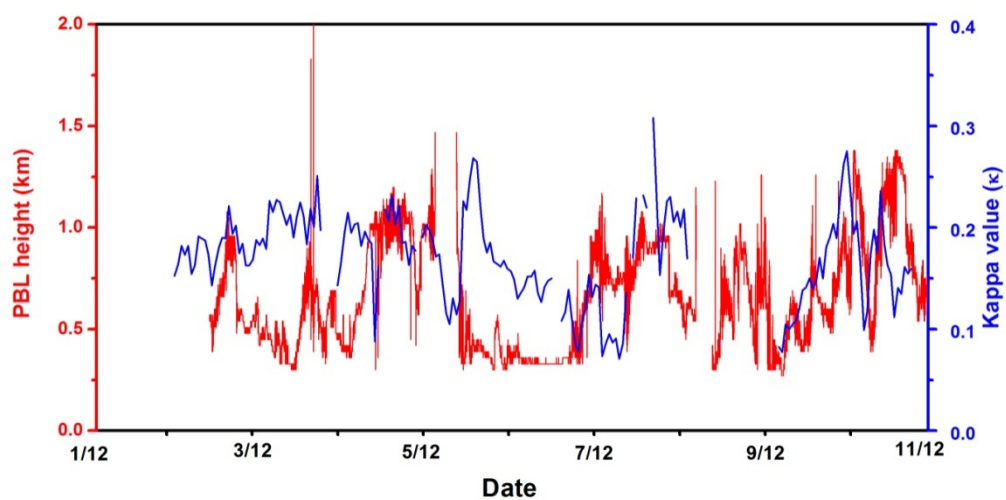


Figure 11 Time series of 1-h mean kappa value (i.e. κ) and 5-min mean PBL height from 1 to 10 December.

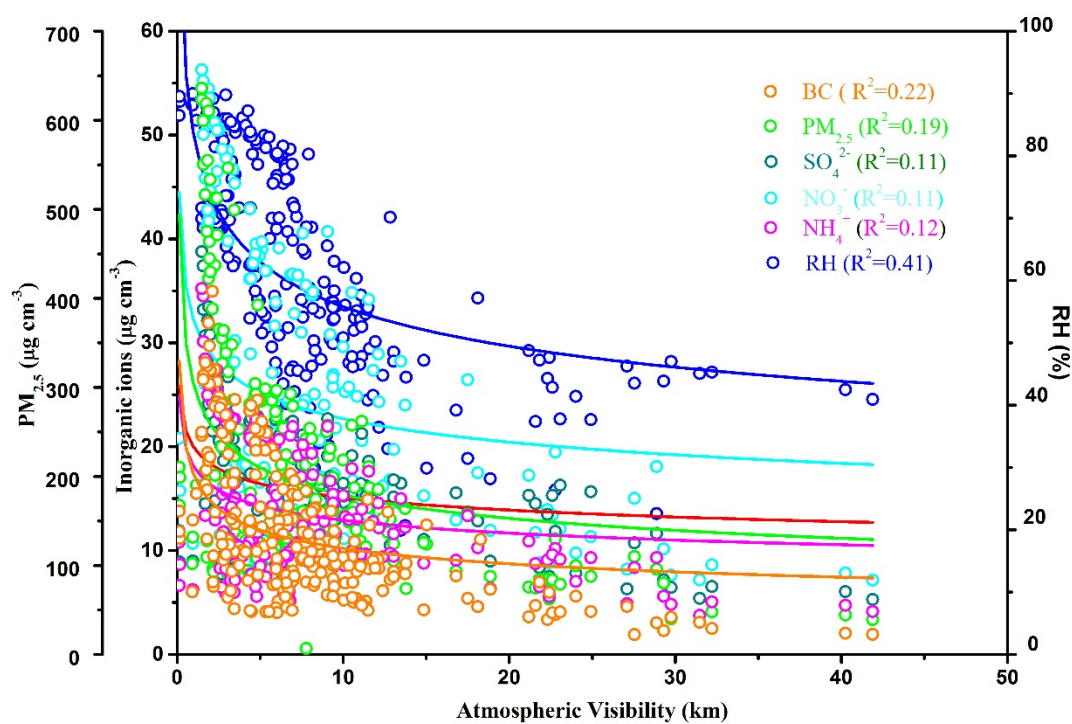


Figure 12 Scatter plots of RH, BC, $PM_{2.5}$ and inorganic ions in particles versus atmospheric visibility.

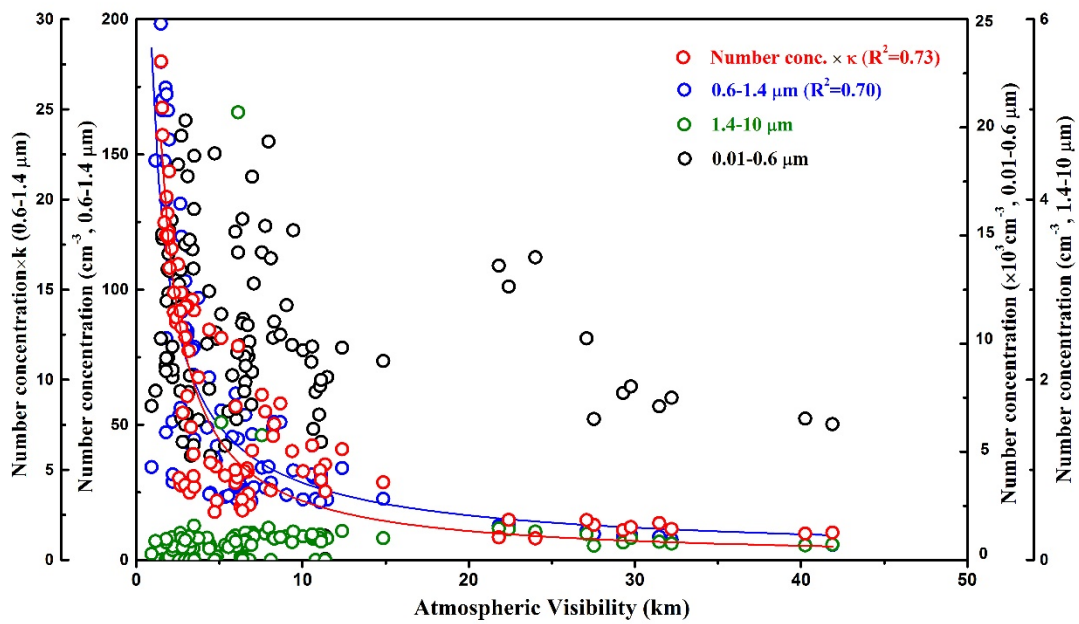


Figure 13 Scatter plots of aerosol number concentrations in ranges of 0.01-0.6 μm, 0.6-1.4 μm and 1.4-10 μm, and aerosol number concentration (0.6-1.4 μm) multiplied by particle hygroscopicity (kappa value, κ) versus atmospheric visibility. (We have just modified the colors in this figure)